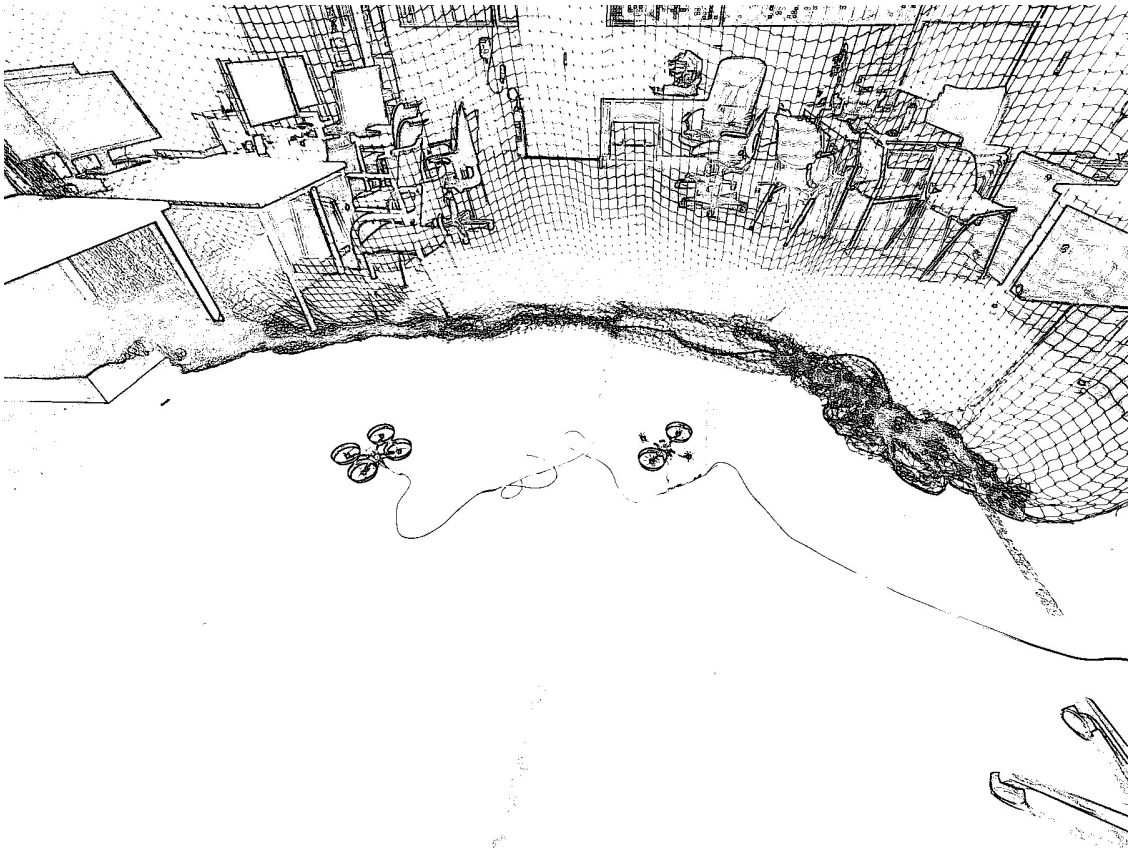

Design of a Complex Tethering System

A prototype of an expandable drone tethering system

Master's thesis in Mobility Engineering, Aerospace track, Msc

Xingyuan Li

DEPARTMENT OF MECHANICS and MARITIME SCIENCES

CHALMERS UNIVERSITY OF TECHNOLOGY
Gothenburg, Sweden 2025
www.chalmers.se

MASTER'S THESIS in Mobility Engineering 2025

Design of a Complex Tethering System

A prototype of an expandable drone tethering system

Xingyuan Li

CHALMERS
UNIVERSITY OF TECHNOLOGY

DEPARTMENT OF MECHANICS and MARITIME SCIENCES
Chalmers University of Technology
Gothenburg, Sweden 2025

Design of a Complex Tethering System
A prototype of an expandable drone tethering system
Xingyuan Li

Supervisor: Arion Pons, Department of Mechanics and Maritime Sciences
Examiner: Fredrik Bruzelius, Department of Mechanics and Maritime Sciences

Degree project report 2025
Department of Mechanics and Maritime Sciences
Chalmers University of Technology
SE-412 96 Gothenburg
Sweden
Telephone +46 31 772 1000

Cover:

Typeset in LaTeX
Gothenburg, Sweden 2025

Design of a Complex Tethering System
A prototype of an expandable drone thethering system
Xingyuan Li
Department of Mechanics and Maritime Sciences
Chalmers University of Technology

Abstract

The dissertation aims to explore a new approach to extend the mission length and expand the flexibility of drone applications for indoor environments where a GPS or GNSS signal is not available. The research addresses the need for enhanced power management and coordinated control in multi-drone systems. A tethering system is created as a prototype to enable simultaneous power distribution and dynamic positioning. Experimental testing was conducted in a controlled lab environment using a linked customized quadcopter and an indoor positioning system. The system demonstrated a complex tethering system with longer durability, higher flexibility, and higher modularity. The prototype provides a foundation for future deployment in a variety of areas including persistent surveillance, emergency communication, indoor manufacturing, and so on. Future work is expected to focus on improving control accuracy and system stability.

Keywords: tethered UAV, multi-drone system, autonomous aerial systems, indoor-positioning

Acknowledgements

I would like to sincerely thank my supervisor, Arion Pons, for his constant support and guidance throughout this thesis. His effort in setting up and maintaining a well-organized lab environment made it much easier to carry out experiments, especially during the more demanding phases of the project. His advice on how to navigate challenges and find practical solutions within limited resources was incredibly valuable—not just for this work, but also as a mindset I'll carry into my professional career. I'm also grateful to my examiner, Fredrick Bruzelius, for his insightful input on control systems, which greatly influenced the development of the control architecture in this project. This experience has been a meaningful step in my growth, and the knowledge and support I've received will stay with me as I move forward into industry.

Xingyuan Li, Gothenburg, Sept.2025

List of Acronyms

Below is the list of acronyms that have been used throughout this thesis listed in alphabetical order:

UGV	Unmanned Ground Vehicle
UAV	Unmanned Aerial Vehicle
UAs	Unamaned Aerial System
PDU	Power Dispatch Unit
AC	Alternating Current
DC	Direct Current
MUAV	Micro UAV
URE	User Range Error
WiFi	Wireless Fidelity
BLE	Bluetooth Low Energy
RFID	Radio Frequency Identification
UWB	Ultrawideband (UWB)
DoF	Degrees of Freedom
PC	PolyCarbonate
PMIC	Power Management Integrated Circuit
LDO	Low-voltage Dropout
PID	Proportional-Integral-Derivative

Nomenclature

Below is the nomenclature of indices, sets, parameters, and variables that have been used throughout this thesis.

Indices

i,j	Indices for distribution network buses
t	Index for time step

Sets

$\mathcal{D}$	Set of distribution network buses
$\mathcal{D}_s$	Set of substation buses
$\mathcal{H}$	Set of time steps (simulation/scheduling horizon)
$\mathcal{N}$	Set of buses

Parameters

γ	Penalty coefficient
Δt	Time discretization step (time interval)
η_j^{ch}	Charging efficiency of BES
η_j^{dis}	Discharging efficiency of BES
$\boldsymbol{H}$	Adjacency matrix
N	Number of iterations
$P_{j,t}^{L}$	Active power of load demand
$P_{j,t}^{PV}$	Active power from solar generation

Variables

p_j	Active power injection at bus j
p_{ji}	Active power flow from bus j to bus i
v_i	Square of voltage magnitude at bus i

Contents

List of Figures

List of Tables

1

Introduction

1.1 Background

General human desires give birth to more and more finely-sorted products, enabling the industries to have increasingly dispersed types of manufacturing facilities for distinct products, ranging from different colors and sizes of mug cups to customized paintings on cars or houses. Nowadays, those demands for more flexibility in manufacturing facilities are a large market for technology development, while due to such indoor applications and requirements for high precision and high flexibility at the same time, there exist limited solutions. One of the most cost-effective idea is to use current existing infrastructures to build a mechanical layer over it to facilitate the functionalities of flexibly disperse manufacturing, such as UGVs equipped with robot hands which take advantage of the flexibility in a large two-dimensional space, or drones equipped with unsimilar end-modules for different end implementations which exploit the resilience of a broad three-dimension space. Relatively, UGVs equipped with an industry-standard robot hand would be less cost-effective, although it might bring higher precision in the end. Since indoor UAV implementations usually do not require any new infrastructure to be additionally constructed, and the comparatively low-precision can be compensated by advanced algorithms during installation, it could be a good way to meet the future needs of manufacturing. While considering drones to solve such problems, it is obvious that the drone itself has several inherited problems regarding operation time, relative stability, precise localization, and human collisions. Those are usually the main challenges during long-term applications in real life. Then, it is not hard to consider methods like charging the UAV continuously or using a better fuel for the UAV to provide a longer operational time. Since current battery technologies are generally limited due to relatively low energy density, finite cycle life, and material-related safety constraints, it would be hardly possible to use common lithium-ion batteries which usually have an energy density of 250 – 300 Wh/kg for long-term operation of drones which equipped with motors that consume high power. Although it is possible to have some weight trade-offs for increasing operation time, the system will be clumsy and unnecessarily large, and harder to implement. Therefore, connecting a power cable to one drone or multiple drones becomes a reasonable solution for long-term applications like surveillance, mapping, and indoor manufacturing. In addition to a continuous power supply, a tethered drone system connected with each other offers potential advantages in terms of improved safety, reduced downtime, and increased payload flexibility.

1.2 Purpose

Despite the rapid development of UAS across various sectors—including commercial, industrial, and military applications—there remains an absence of tethered UAV systems specifically designed for indoor environments with fully autonomous operation both vertically and horizontally. While tethered drones have demonstrated significant potential in addressing limitations related to battery life and data latency in outdoor settings, their adaptation for indoor autonomous applications is still underexplored. Addressing this gap, the primary aim of this research is to design and develop a functional prototype of an expandable tethered drone system tailored for indoor deployment. In the course of system development, a novel implementation framework was introduced to support modularity and scalability, enhancing the system's adaptability to diverse operational scenarios. The development process emphasizes the integration of existing commercial components and prototype technologies, demonstrating not only the technical feasibility of such a system but also its potential for future enhancement and deployment. This study validates the proposed tethered UAV architecture through extensive hardware implementation and iterative flight testing conducted over several months in a controlled laboratory setting.

1.3 Objectives

To design and build a functional tethered drone power system, several different goals have been set:

- **Component Selection:** Identify and select reliable commercial and custom components suitable for a tethered UAV system, with a particular focus on efficient and stable power transmission through the tethering cable.
- **System Customization:** Appropriately adapt or modify critical hardware and software components to meet the unique requirements of tethered drone operation in constrained environments.
- **Implementation structure:** Develop a general implementation structure for such a tethered drone system in a controlled environment in the absence of GPS or GNSS.
- **Prototype Development and Deployment:** Construct a modular and expandable tethered drone prototype and demonstrate its operational feasibility in a controlled real-time environment. This includes the integration and validation of the following subsystems:
  - **Power Supply System:** Choose a robust and high-capacity power delivery infrastructure capable of continuous operation, ensuring minimal energy loss over the tether.
  - **Safety-Oriented Drone Structure:** Design a mechanical frame and enclosure that minimizes risk to humans and surroundings, particularly by safeguarding against exposed propellers during indoor operation.
  - **Onboard Power Management:** Implement a reliable onboard power

distribution unit (PDU) to supply clean and consistent power to flight controllers, sensors, and peripheral components.
- **Control Software Integration:** Tune and adapt flight control algorithms to accommodate the physical constraints imposed by tethered flight, ensuring stable and responsive maneuverability under variable tether tension.

1.4 Limitations

This dissertation primarily focuses on the development and evaluation of a tethered UAV system within a controlled indoor environment. Consequently, the results and conclusions may not be directly generalizable to outdoor or highly dynamic operational scenarios. The current system does not include autonomous tether management or obstacle avoidance capabilities, as the primary objective was to demonstrate the feasibility of a basic tethered UAV architecture for constrained indoor settings such as chemical laboratories or manufacturing facilities. Human safety considerations are addressed through passive design strategies, such as mechanical fail-safes, rather than active collision avoidance systems. Besides, Aerodynamic analysis is limited to general efficiency considerations; detailed modeling and analysis of aerodynamic effects, particularly those arising from interactions between multiple UAVs, are beyond the scope of this work. Due to time and resource constraints associated with the scope of a master's thesis, which spans two academic semesters, aspects such as multi-drone power distribution scalability, tether tension control, and inter-UAV avoidance algorithms have not been explored. Also, potential power loss along longer tethers has not been thoroughly investigated, as the system was designed for short-range applications. The selection of tether materials was made based on availability and pragmatic trade-offs between weight, flexibility, and electrical conductivity, without extensive optimization. Moreover, the current system lacks real-time tether tension control, relying instead on a passive tether configuration, which may limit stability and safety in more complex environments. These constraints are acknowledged as areas for future research and development.

2

Literature Review

With rapid advancements of UAVs in recent years, a variety of types of UAS have been implemented in various fields, including industrial inspection, logistics, surveillance, and scientific research. While common battery-powered drones have become increasingly capable, their operational endurance remains inherently limited by energy storage constraints, posing challenges for long-duration missions, especially in confined indoor environments. Tethered UAS, which draw continuous power from a ground station that could be a large PDU that transfers common AC power to DC for the UAS or a battery-based station, provide a viable solution for extending flight time and improving operational safety. However, most existing research and commercial systems are optimized for outdoor, stationary applications and rarely address the complexities of indoor deployment and modular scalability. This literature review examines the current state of tethered UAV technologies with emphasis on power transmission, cable management, localization, and system integration. The review establishes a foundation for the design and development of the tethered UAV prototype presented in this thesis by identifying technological gaps in existing approaches, particularly regarding flexible, expandable indoor systems.

Although the concept of the tethered aerial system explored in this study draws inspiration from the researcher's background in mechatronics engineering, the fundamental idea of utilizing a physical tether to connect and control a vehicle dates back to early military innovations, notably the Brennan torpedo in the late 19th century [1]. In this historical instance, the tether—essentially a wire—was employed for propulsion and directional control. Over the decades, with the advancement of robotics and control systems, tethered systems have evolved to serve a range of functions across different domains. One of the earliest and most enduring applications can be found in underwater robotics, where radio frequency (RF) communication is severely limited. Consequently, tethers have been extensively used for both data communication and power supply in underwater vehicles. For example, a lightweight tether system was demonstrated in [3] to enable extended-range communication and control, while [2] presented a fiber-optic tethered autonomous underwater vehicle for real-time surveillance and data transmission. Beyond underwater domains, tethered systems have also been applied in aerial contexts. In [4], a tether was utilized to enhance the stability of airships by providing mechanical anchoring and control. Furthermore, the use of tethered connections for data monitoring and communication in aerial vehicles has been investigated in studies such as [8] and [9], highlighting the growing interest in persistent and reliable links between ground stations and

flying platforms. In the realm of vertical take-off and landing (VTOL) unmanned aerial vehicles (UAVs), tethered systems have primarily been explored for continuous power delivery, as demonstrated in works such as [5], [6], and [7]. However, most of these implementations are constrained to micro-UAVs or mini-UAVs, delivering power levels typically below 200W. As a result, such systems are not equipped to carry significant payloads—often limited to less than the equivalent of a 500 mL water bottle—thereby restricting their utility in more demanding operational scenarios.

While much of the prior work emphasizes power delivery and data transmission via tethered cable, these solutions often assume outdoor environments where GPS or GNSS are available. However, in indoor settings like the Chalmers Wind-tunnel or any underground laboratories, GPS or GNSS signals are usually unavailable or unreliable, making precise localization and navigation for UAV operations difficult. Therefore, indoor positioning plays a very important role in it. Indoor positioning technologies can be separated into seven main categories.

1. **Satellite-based positioning system**
   GPS is the most common satellite-based positioning system in people's daily lives, providing users with an approximately average URE of less than 7.8 meters 95 percent of the time, anywhere on or near the surface of the earth [10]. Despite the ease of the implementation of GPS, it is hard to get a centimeter-level accuracy for indoor applications.
2. **Magnetic-based positioning system**
   Magnetic-based positioning system can either make use of anomalies induced by disruptions in the earth's magnetic field to give the position of a thing, or it can use certain artificially generated magnetic fields in which coils of current-carrying wire are installed in strategic areas throughout the structure [11]. Magnetic-based system usually requires relatively complex infrastructure work before the system can be calibrated and used smoothly.
3. **Inertial sensor-based positioning system**
   Sensor-based positioning system depends on one or multiple inertial sensors to detect the relevant movement of the object from the start. Those sensors mainly include accelerometers and gyroscopes. However, to get very accurate readings from the sensor requires a certain trade-off in cost and internal algorithms of the embedded system.
4. **Sound-based positioning system**
   There are three types of sound-based positioning systems which are audible sound-based, ultrasonic sound-based, and acoustic sound-based. Audible sound-based systems use frequencies within the human hearing range and are relatively easy to implement, but are vulnerable to ambient noise and interference [12]. Ultrasound-based systems, which operate above 20 kHz, offer higher accuracy due to slower sound speed in air and are widely used for indoor localization, though they suffer from short range and line-of-sight constraints [13]. Acoustic methods at lower frequencies are mainly employed in underwater or underground environments, where radio signals fail [14]. Such technology is quite sensitive to environmental changes and noises, and in lack of certain accuracy regarding our applications.

5. **Optical-based**
   Optical-Based positioning used for localization is normally in the form of an Electro-Magnetic (EM) spectrum. One of the cost-effective and extensively used options is an infrared-based positioning system [15]. There are also existing products like SteamVR that implement infrared positioning technology to improve the interactions between machines and humans.
6. **Radio frequency-based**
   Radio frequency-based positioning systems can be separated into four categories: WiFi-based, BLE-based, RFID-based, and UWB-based systems. Wi-Fi is commonly used for indoor positioning due to its widespread infrastructure. However, its performance suffers from fluctuating signal strengths and multipath interference, typically providing room-level accuracy (5–15 m) [16]. BLE is cost-effective and energy-efficient, offering moderate accuracy (1–5 m). It is suitable for proximity-based applications, though its performance is sensitive to obstructions and device placement [17]. RFID is often used in logistics and asset tracking. Passive RFID is inexpensive but limited in range and granularity, while active RFID systems offer better performance at a higher cost [18].UWB provides high-resolution positioning (10–30 cm), excellent performance in non-line-of-sight conditions, and low interference. However, it requires specialized infrastructure and is relatively costly [19].
7. **Vision-based**
   Vision-based system depends on multiple cameras in an indoor environment, and usually those cameras are fixed in certain corners inside a room although there were implementations with multiple movable cameras[20]. However, the accuracy of such system is highly based on the pixel resolution of the camera, meaning a cost trade-off in our application for small-sized drones in low speed.

The absence of reliable satellite signals in indoor environments necessitates the adoption of specialized positioning technologies tailored to these conditions. Each indoor positioning system category offers distinct advantages and challenges concerning accuracy, infrastructure requirements, cost, and robustness to environmental factors. Consequently, careful evaluation and selection of the most suitable positioning solution are imperative to ensure precise and reliable UAV localization and navigation within GPS-denied indoor settings such as wind tunnels and underground laboratories.

In summary, tethered UAV systems offer a viable approach to overcoming the intrinsic limitations of battery-powered drones by enabling continuous power supply and enhanced operational endurance, which are particularly critical for prolonged indoor missions. However, extant research predominantly focuses on outdoor or stationary applications, where reliable satellite-based positioning systems such as GPS or GNSS are available. The indoor environment, characterized by the absence or degradation of such satellite signals, introduces significant challenges for UAV localization and navigation, necessitating the deployment of alternative indoor positioning technologies. This review has systematically examined seven principal categories of indoor positioning systems each presenting unique advantages and inherent limitations with respect to accuracy, infrastructure complexity, cost, and environmental

susceptibility. Despite the breadth of existing approaches, there remains a conspicuous gap in the integration and scalability of these systems tailored specifically for tethered UASs within confined or complex indoor spaces such as underground laboratories and manufacturing facilities. Therefore, further research is to have modular and cost-effective positioning solutions that can be seamlessly integrated with tethered power delivery mechanisms. This foundational understanding will inform and guide the design and implementation of the tethered UAS prototype explored in this thesis.

3

Design of the tethering system

3.1 Overview

This prototype design of the complex tethering system was mainly to prove the feasibility of a solution that is inspired by the relevant market needs in the industry, including a continuous power supply for long-duration missions and a precise positioning system in GPS-limited or GNSS-limited areas. Thus, the prototype system consists of three main components: a good PDU for power transmission from the AC civil power supply or the industry three-phase AC power supply, a cable that is good enough to sustain the heat and with low power-lost, a drone or multiple drones that are small but big enough to lift a reasonable payload. The framework of the tethering system should be designed as the picture below:

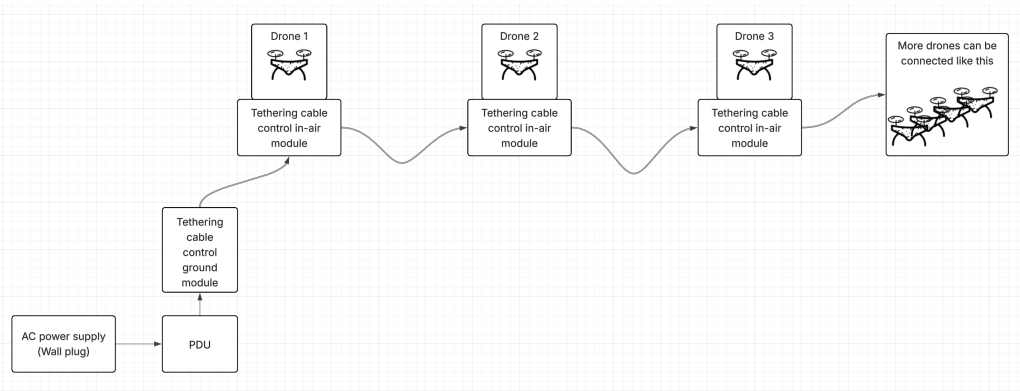

Figure 3.1: General Framework

However, due to the limitation of time and resources during the master's thesis, a simplified framework is created:

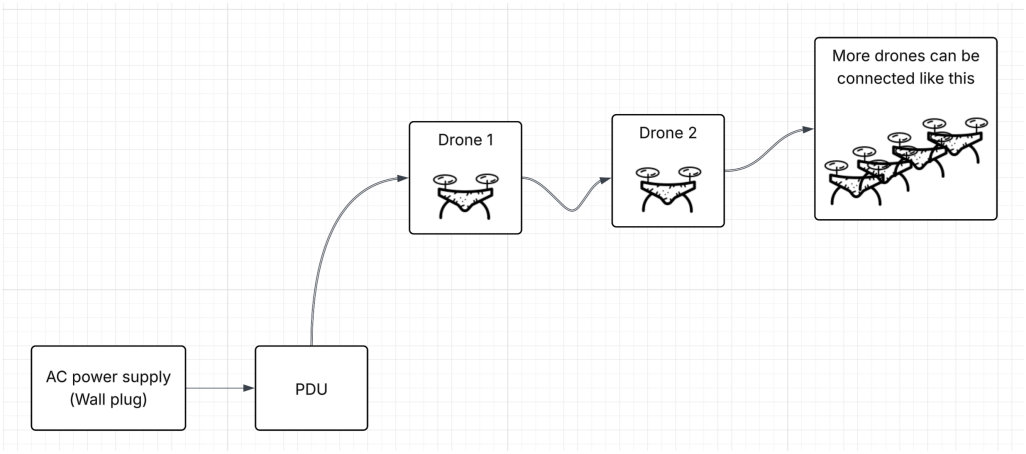

Figure 3.2: Simplified Framework

The tethering control system is not the main area of this dissertation, but the system integration of the complex tethering system, of which the PDU can be paralleled according to power requirements and the number of drones, and the drones can be connected one to another according to the requirements of the mission.

Along the development of the tethering system, several key subsystems were either designed from scratch or carefully integrated to achieve a functional and modular architecture. These include the ground-based power supply unit, the onboard power conversion and regulation module, the selection of the tethering cable, the mechanical structure and safety design of the drone, as well as the control and communication frameworks required for stable operation. Each subsystem was developed with the overarching goal of system modularity and user flexibility in mind. The architecture allows end-users to easily modify or scale the system by selecting an appropriate number of drones or customizing the onboard power distribution units (PDUs) according to specific mission requirements. This modular approach not only facilitates future expansion and maintenance but also enables adaptation to various operational scenarios, such as indoor inspection, monitoring, or research activities in constrained environments.

3.2 Components selection

3.2.1 Requirements

The primary functional requirement of the tethered UAV system is to transport a payload of moderate mass—approximately 500 grams—between two locations within an indoor environment. This scenario imposes specific design constraints related to lift capacity, spatial maneuverability, and power efficiency. Given that the estimated mass of the drone platform itself is approximately 350 grams, the total takeoff weight becomes roughly 850 grams. In typical multirotor UAV design, a maximum thrust-to-weight ratio of 4:1 to 5:1 is generally recommended to ensure sufficient control authority, maneuverability, and flight stability, especially in

confined or obstacle-rich environments. Accordingly, the system must be capable of generating a maximum thrust in the range of 3.5 to 4.5 kilograms. At the same time, the compact nature of indoor spaces—such as laboratory or manufacturing environments, necessitates a minimized drone footprint. This constraint requires the use of smaller propellers, which in turn affects propulsion efficiency and demands higher motor rotational speeds to achieve the necessary lift. Moreover, to optimize the efficiency of electrical power delivery through the tether, a higher voltage power transmission scheme is preferred. Operating at elevated voltages reduces the current draw, thereby minimizing resistive losses along the tether and enhancing the overall stability and reliability of the power supply to the onboard systems. These interdependent design considerations form the foundation for the selection and integration of mechanical, electrical, and control subsystems within the proposed tethered UAV architecture. Therefore, the sequence selection should be from propeller and propulsion, to electrical components and power supply.

3.2.2 Motor selection

Several brands of motor have been selected:

1. RCinpower SmooX1507 plus 2680kv

Figure 3.3: Rcinpower SmooX1507

- Motor weight: 16.8 g
- Max current rating: 19A
- Voltage: 6s Lipo
- Max static thrust with four-inch (QF4030-3) propeller: 1101 g
- Current at maximum thrust: 18.9 A
- Thrust at half-throttle: 458 g
- Current at half-throttle: 4.4 A
- Average efficiency: 3.6 g/w

2. T-motor F1507 2700kv

Figure 3.4: T-motor F1507

- Motor weight: 15.2 g
- Max current rating: 22 A
- Voltage: 6s Lipo
- Max static thrust with three-inch (T3140-3) propeller: 838.7 g
- Current at maximum thrust: 23.34 A
- Thrust at half-throttle: 286.38g
- Current at half-throttle: 5.12 A
- Average efficiency: 2.1 g/w

3. AMAX 2005 2500kv

Figure 3.5: AMAX 2005

- Motor weight: 21 g
- Max current rating: 30 A
- Voltage: 6s Lipo
- Max static thrust with four-inch (T4025-3) propeller: 1152 g
- Current at maximum thrust: 16 A
- Thrust at half-throttle: 638 g
- Current at half-throttle: 7 A
- Average efficiency: 3.2 g/w

Those three motors all satisfied the initial requirements for this prototype. However, it is obvious that they have quite different throttle curves, thus, we need some later test to know which one will sustain us to the last.

3.2.3 ESC selection

After selecting three candidate motor types, the next step involves identifying compatible Electronic Speed Controllers (ESCs) that align with the operational requirements of the system. The chosen ESCs must support a 6S LiPo battery configuration and be compatible with flight controllers that operate at high main clock speeds, ensuring fast and reliable signal processing. One of the critical considerations in ESC selection is the current handling capacity. Since the burst current during motor operation—particularly under high-load or locked-rotor conditions—can exceed the nominal current rating by up to two times, it is essential to choose ESCs with sufficient current tolerance and thermal protection mechanisms. ESCs are generally considered consumable components in UAV systems, as they are more likely to fail than motors under fault conditions. This is especially relevant during the prototyping and tuning phases, where frequent changes in parameters or control logic may cause unexpected behavior. For example, if a quadcopter crashes or a rotor becomes locked, the motor may draw excessive current, leading to ESC burnout. Therefore, considering the cost-effectiveness, the following ESCs are selected:

1. Speedybee 35A 4-in-1 ESC
2. Speedybee 55A 4-in-1 ESC
3. XRotor Micro 40A 4-in-1 ESC

All three ESC options satisfy the predefined selection criteria, including compatibility with the power system and flight controller, as well as appropriate current ratings. However, similar to motor specifications, the manufacturer-provided performance parameters may not fully reflect real-world behavior under the specific operating conditions of this system. Therefore, empirical testing and comparative evaluation are necessary to assess their actual performance in practice. Through iterative testing and integration within the prototype, the final ESC will be chosen during the testing process.

3.2.4 Flight controlling system selection

As discussed in the preceding chapter, satellite-based positioning systems such as GPS are unsuitable for indoor environments due to significant signal attenuation and unavailability within enclosed spaces. Similarly, sound-based localization methods—including ultrasound and acoustic techniques—are not ideal for this application, given the shared nature of the laboratory environment, which introduces high levels of acoustic interference from human activity and machinery. Considering these constraints, along with the available resources and budgetary limitations of the project, an optical positioning approach is deemed more appropriate. In particular, infrared-based positioning systems present a viable and cost-effective solution for reliable indoor localization in this context. According to personal experience, there are two types of infrared-based positioning system we can choose. One is a motion-caption system. The other one is an indoor infrared scanning system. The first one usually requires more infrastructure then the second one, so it is quite costly. Therefore, the Bitcraze lighthouse positioning system is chosen. It includes two parts: the base station, and the lighthouse positioning deck that is installed on the quadcopter, combined with the Crazyflie Bolt flight controller. The system uses infrared laser sweeps emitted by the Lighthouse Base Stations (v1 or v2). These sweeps are received by an array of light sensors mounted on the Crazyflie, which measure the timing and angle of the incoming signals. Using time difference of arrival (TDoA) and angle data, the onboard algorithm computes the drone's precise 3D position and orientation in space. Compared to traditional UWB systems like Bitcraze's Loco Positioning System, the Lighthouse system is more compact with no additional anchors or infrastructures beyond the base stations, highly accurate for millimeter-level precision, and scalable for larger areas[21].

3.2.4.1 Bitcraze Lighthouse positioning system

Here is a concept piture of the positioning system.

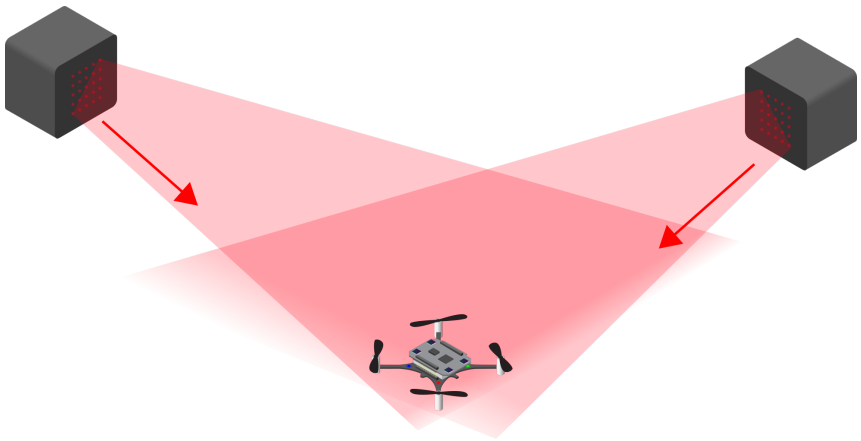

Figure 3.6: Lighthouse positioning system

It simply consists of two or multiple base stations which emit a stable frequency of infrared light sweep, and the deck onboard with 4 sensors (photodiode) will calculate

the positions relevant to the pre-calibrated area. Each lighthouse base station emits a synchronization flash (broad IR pulse), followed by laser sweeps in two perpendicular directions (horizontal and vertical). Each sensor (photodiode) on the deck will record the timestamp of the sync pulse, and wait for the timestampe of the sweep crossing. From those data, the angular position of each sensor with respect to the base station is calculated as:

$$\theta = (t_{\text{sweep}} - t_{\text{sync}}) \cdot \omega \tag{3.1}$$

where:

- t_{sync} is the timestamp of the synchronization pulse,
- t_{sweep} is the timestamp when the laser sweep hits the sensor,
- ω is the angular velocity of the lighthouse laser (in radians per second),
- θ is the resulting angular position of the sensor relative to the base station.

After each base station gives two angles for every photodiode. These angles define the direction vectors from the base station toward each sensor on the drone. Through the pre-calibration process, the base stations' positions are known.

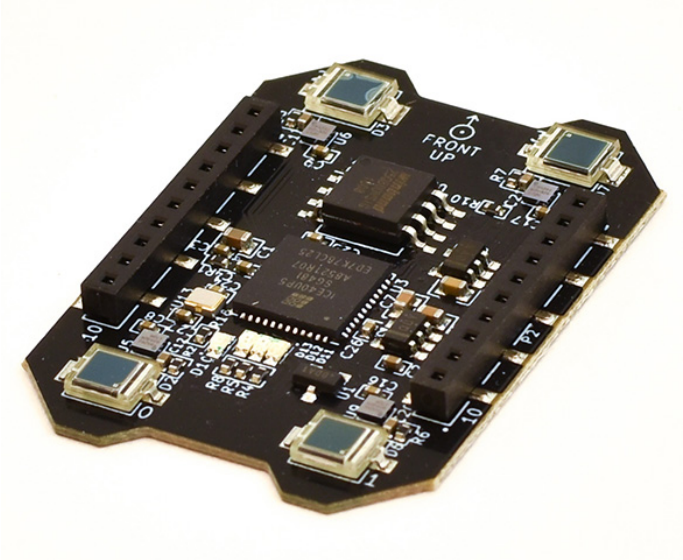

Figure 3.7: Lighthouse positioning deck

The Bitcraze's firmware then uses a nonlinear least-squares optimization approach to minimize the angular error between expected and observed beam directions. The optimization estimates the drone's pose by solving:

$$\min_{\mathbf{R},\mathbf{t}} \sum_i \left\| \frac{\mathbf{R}\mathbf{p}_i + \mathbf{t}}{\|\mathbf{R}\mathbf{p}_i + \mathbf{t}\|} - \hat{\mathbf{d}}_i \right\|^2 \tag{3.2}$$

where:

- $\mathbf{p}_i$ is the known position of sensor i in the drone's body frame,
- $\hat{\mathbf{d}}_i$ is the unit vector direction from the base station to the sensor (measured),
- $\mathbf{R}$ is the rotation matrix representing the drone's orientation,
- $\mathbf{t}$ is the translation vector representing the drone's position,

- $\mathbf{R}\mathbf{p}_i + \mathbf{t}$ transforms the sensor's local position into the world frame.

This kind of optimization is usually solved using methods like Levenberg-Marquardt, which are effective for pose refinement in rigid-body transformations [22]. The estimated pose is then fused over time using an Extended Kalman Filter, which integrates IMU data to smooth noise and improve robustness under occlusion or temporary signal loss.

In reality, the base stations are initially installed in my garage and the base stations look like as the follow:

Figure 3.8: SteamVR base station

Figure 3.9: Installed base station

3.2.4.2 Bitcraze CrazyBolt Flight Controller

Because of the convenience of the CrazyFlie eco-system, the CrazyBolt flight controller is chosen for the custmized quadcopter. The Crazyflie Bolt 1.1 is an open-source, brushless flight controller developed by Bitcraze, designed to bring the flexibility and modularity of the Crazyflie 2.X ecosystem to larger and more powerful drones. It supports 1–4S LiPo batteries and features integrated ESC connectors for brushless motors, allowing for high-thrust applications but based on our motor choices, some minor change with it will be needed.

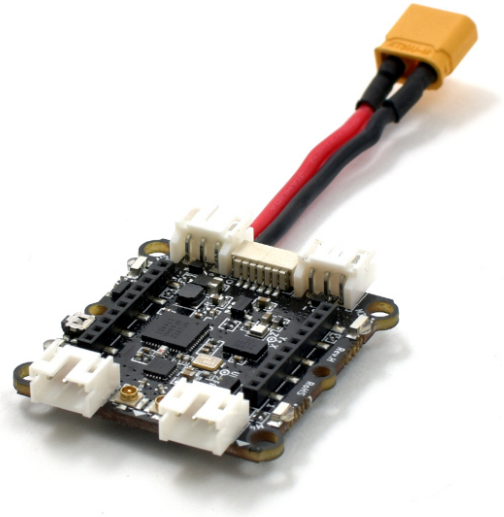

Figure 3.10: CrazyBolt Flight Controller

3.2.5 Cable selection

For the main power transmission line of the tethered UAV system, a high-temperature silicone-insulated 12 AWG high temperature silicone cable has been selected. This choice is grounded in the need to balance current-carrying capacity, thermal stability, mechanical flexibility, and weight. The 12 AWG cable offers a practical compromise, capable of safely carrying continuous currents in the range of 50–60A with minimal voltage drop over moderate lengths, which aligns with the system's 24V supply and peak load demands. According to the manufacturer, a table of different size of silicone cables and the respectively current and power ratings are shown.

Cable Number	Diameter (mm)	Resistance (ohms/km)	Cross-section area (mm^2)	Nominal Current (A)
6 AWG	8.5	1.21	16.08	300
8 AWG	6.3	4.1	8.29	190
10 AWG	5.5	6.3	5.3	140
12 AWG	4.5	9.8	3.4	132
14 AWG	3.5	15.6	2.07	82.5
16 AWG	3.0	24.4	1.27	55.6
18 AWG	2.3	39.5	0.75	22
20 AWG	1.8	62.5	0.5	13.87
22 AWG	1.7	88.6	0.33	8.73
24 AWG	1.6	97.6	0.2	5

Based on the power requirements for the dual-drone configuration, the maximum nominal current for the tethered power supply is estimated by assuming two-thirds of the full-throttle current, to ensure sufficient power delivery under typical high-load conditions without significant voltage drop. Each quadcopter is equipped with four motors, each drawing a peak current of approximately 20A. Therefore, the combined nominal current for both drones is calculated to be around 106A. To maintain a balance between electrical performance and mechanical feasibility, a lightweight cable solution is preferred. Under this constraint, 12 AWG wire is considered adequate for this application, as it provides acceptable current-carrying capacity over short distances typical of indoor use, while minimizing added weight and drag.

Additionally, silicone-insulated multi-strand wires were selected over standard single-core or thermoplastic-insulated alternatives. Silicone offers superior thermal resistance, typically up to 200°C, and maintains its structural integrity under elevated temperatures where conventional plastic insulation may degrade, melt, or burn and causing fire. Given the experimental nature of the prototype and the potential for momentary current surges beyond nominal ratings, the use of silicone-insulated wire enhances system safety and reliability during prolonged testing or fault conditions.

3.2.6 PDU selection

In the design of a tethered UAV system, the Power Distribution Unit (PDU) plays a critical role in delivering continuous and stable power from the ground to the airborne platform. For this project, a parallelable 4kW DC power supply was selected, operating at approximately 24V to match the UAV's 6S LiPo-equivalent voltage level. In order to deliver stable power to two drones in parallel, 4kw of power will be initially estimated to be needed becasue one motor usually have a maximum power of about 500w or even more, then, two drones with eight motors will need at least 4kw of power. While with the increase of need of the number of drones, the power supply can be paralleled, this can satisfy later integration requirements. Therefore, a power supply with a stable of 4kw output at 24v will be needed, and MeanWell RST-5000-24 PDU will be chosen.

SPECIFICATION

MODEL		RST-5000-24	RST-5000-36	RST-5000-48
OUTPUT	DC VOLTAGE	24V	36V	48V
	RATED CURRENT	200A	138A	105A
	CURRENT RANGE	0 ~ 200A	0 ~ 138A	0 ~ 105A
	RATED POWER	4800W	4968W	5040W
	RIPPLE & NOISE (max.) Note.2	150mVp-p	200mVp-p	200mVp-p
	VOLTAGE ADJ. RANGE	23.5 ~ 28.8V	35 ~ 43.2V	47 ~ 57.6V
		Can be adjusted via built-in potentiometer		
	VOLTAGE TOLERANCE Note.3	±1.0%	±1.0%	±1.0%
	LINE REGULATION	±0.5%	±0.5%	±0.5%
	LOAD REGULATION	±0.5%	±0.5%	±0.5%
	SETUP, RISE TIME	2200ms, 80ms at full load		
	HOLD UP TIME (Typ.)	20ms / 230VAC at 75% load 14ms / 230VAC at full load		
INPUT	VOLTAGE RANGE	3 ϕ 3-wire / △ 196 ~ 305VAC or 3 ϕ 4-wire / Y 340 ~ 530VAC		
	FREQUENCY RANGE	47 ~ 63Hz		
	POWER FACTOR (Typ.)	0.95/230VAC(400VAC) at full load		
	EFFICIENCY (Typ.)	88.5%	89.5%	90.5%
	AC CURRENT (Typ.)	15A/230VAC(3 ϕ 3-wire / △) 9A/400VAC(3 ϕ 4-wire / Y)		
	INRUSH CURRENT (Typ.)	75A/230VAC(3 ϕ 3-wire / △) 50A/400VAC(3 ϕ 4-wire / Y)		
	LEAKAGE CURRENT	<3.5mA / △305VAC(Y 530VAC)		
PROTECTION	OVERLOAD	100 ~ 112% rated output power		
		User adjustable continuous constant current limiting or constant current limiting with delay shutdown after 5 seconds, re-power on to recover		
	OVER VOLTAGE	30 ~ 33.6V	45 ~ 50.4V	60 ~ 67.2V
		Protection type : Shut down o/p voltage, re-power on to recover		
	OVER TEMPERATURE	Shut down o/p voltage, recovers automatically after temperature goes down		
FUNCTION	REMOTE SENSE	Compensate voltage drop on the load wiring up to 0.3V. Please refer to the Function Manual.		
	CURRENT SHARING	Up to 20000W or (3+1) units. Please refer to the Function Manual.		
	OUTPUT VOLTAGE PROGRAMMABLE	Adjustment of output voltage is allowable to between 20 ~ 120% of nominal output voltage. Please refer to the Function Manual.		
	CONSTANT CURRENT LEVEL PROGRAMMABLE	Adjustment of constant current level is allowable to between 20 ~ 100% of rated current. Please refer to the Function Manual.		
	AUXILIARY POWER(AUX)	12V@0.1A(Only for Remote ON-OFF control)		
	REMOTE ON-OFF CONTROL	Please refer to the Function Manual.		
	ALARM SIGNAL OUTPUT	AC fail, DC OK, fan fail, OTP. Please refer to the Function Manual.		
ENVIRONMENT	WORKING TEMP.	-30 ~ +70℃ (Refer to "Derating Curve")		
	WORKING HUMIDITY	20 ~ 90% RH non-condensing		
	STORAGE TEMP., HUMIDITY	-40 ~ +85℃, 10 ~ 95% RH non-condensing		
	TEMP. COEFFICIENT	±0.03%/℃ (0 ~ 50℃)		
	VIBRATION	10 ~ 500Hz, 2G 10min./1cycle, 60min. each along X, Y, Z axes		
	SAFETY STANDARDS	UL62368-1, CAN/CSA C22.2 No. 62368-1, TUV BS EN/EN62368-1, EAC TP TC 004 approved		
	WITHSTAND VOLTAGE Note.4	I/P-O/P:3KVAC I/P-FG:2KVAC O/P-FG:0.5KVAC		
	ISOLATION RESISTANCE Note.4	I/P-O/P, I/P-FG, O/P-FG:100M Ohms / 500VDC / 25℃/ 70% RH		

Figure 3.11: PDU specifications

Figure 3.12: PDU selection

3.3 Drone design

To develop a customized UAV platform tailored for a tethered indoor drone system, several key design considerations were prioritized. First, the UAV must be compact enough to operate safely within constrained indoor environments. Second, the structural configuration should be designed to minimize the risk of injury in the event of a collision, making safety in human-drone interaction a primary concern. Third, the frame should be sufficiently robust to withstand frequent low-altitude crashes that may occur during development and testing. Compatibility with commonly used flight controllers and electronic speed controllers (ESCs) was also ensured by adhering to industry-standard mounting dimensions (20mm $\times$ 20mm with M2.5 screws or 30.5mm $\times$ 30.5mm with M3 screws).
In terms of safety and aerodynamic efficiency, ducted propeller guards were integrated into the drone frame. These ducts serve not only to shield users from potential injuries caused by exposed rotating propellers but also to enhance airflow control and thrust efficiency in close-proximity environments. Design guidelines were referenced from established works, including [25] and [26], which suggest that duct geometry, clearance, and length significantly influence aerodynamic performance and propeller wash characteristics [23] and [24].
Additionally, to support indoor localization using a Lighthouse tracking system, the lighthour positioning deck was placed on top of the frame to ensure optimal line-of-sight visibility. Unlike conventional FPV drone configurations, this design is purposefully modified to accommodate both the localization system and the control system. To facilitate rapid prototyping and structural integrity, the drone frame was fabricated using polycarbonate (PC) filament with in-house FDM 3D printing, offering a favorable balance between durability, weight, and ease of manufacturing. This is a decision during the relatively long lead time of the carbon fiber board cutting. The inital design looks like the following:

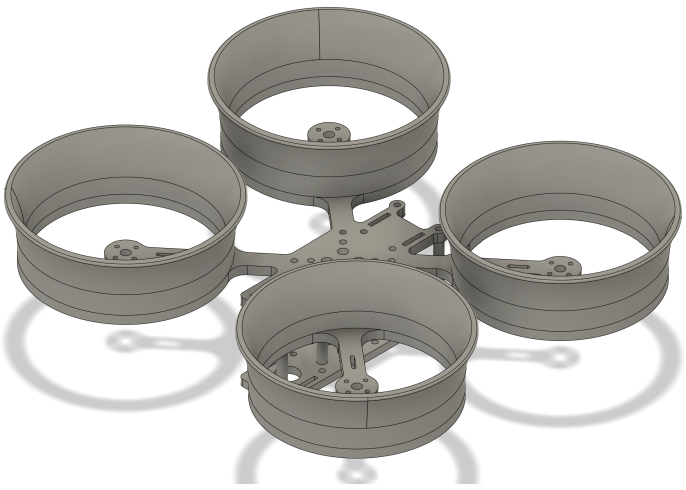

Figure 3.13: 3D-printed version

The drawing of the upper part is shown as the following:

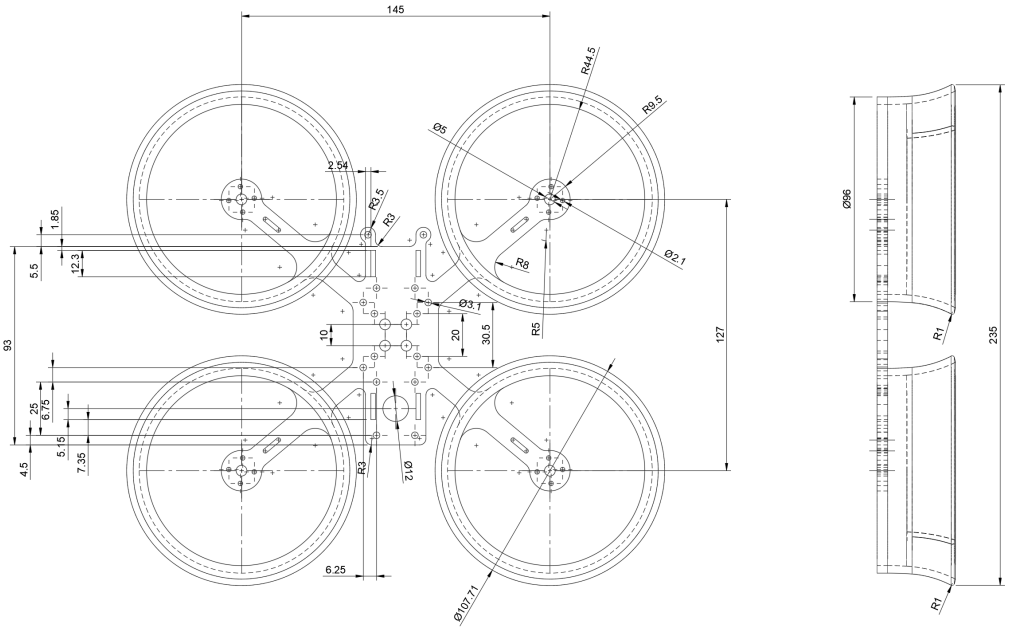

Figure 3.14: The upper part drawing

The initial assembly of the drone is shown as the following:

Figure 3.15: Initial Assembly

Subsequently, a carbon fiber variant of the drone was developed, maintaining the

original dimensional specifications. In this revised design, the duct structure was modularized, and a protective landing gear was designed to be broken first in crashes, which will protect the sensors on board. This enhancement aims to reduce the risk of processor malfunction during high-G impact events, such as crashes.

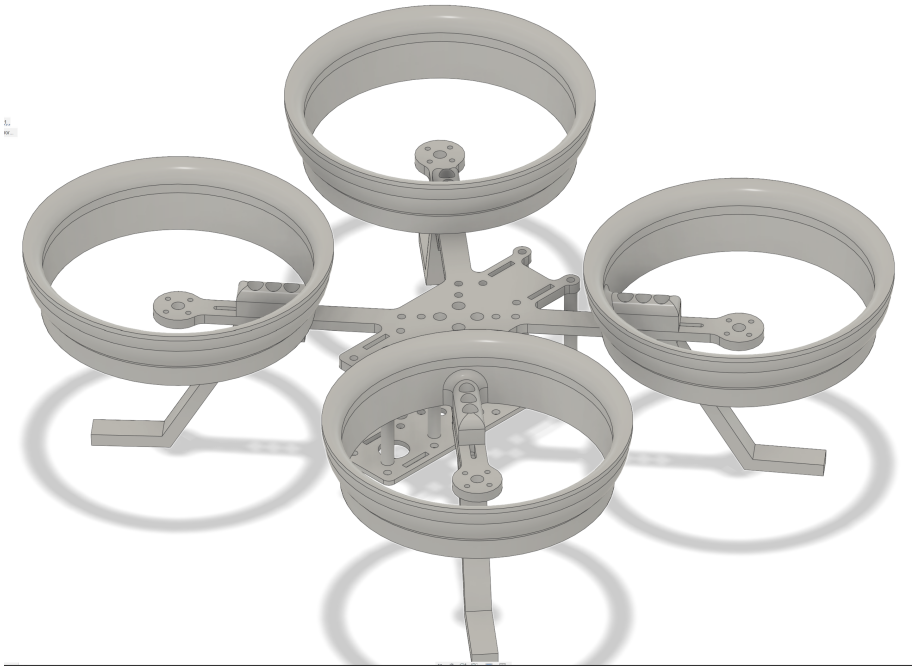

Figure 3.16: Carbon-fiber version of the tethering drone-3D CAD

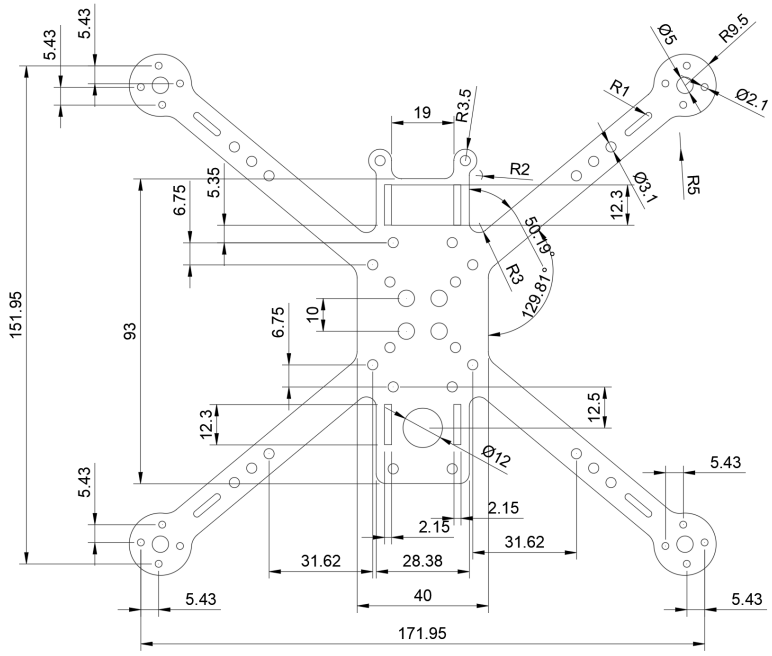

Figure 3.17: Main board drawing

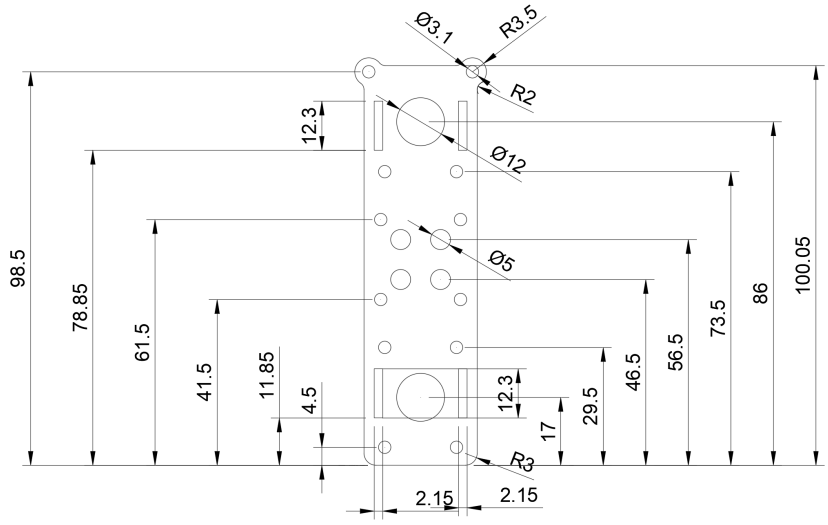

Figure 3.18: Second board drawing

The duct and the gear is separately designed as the following:

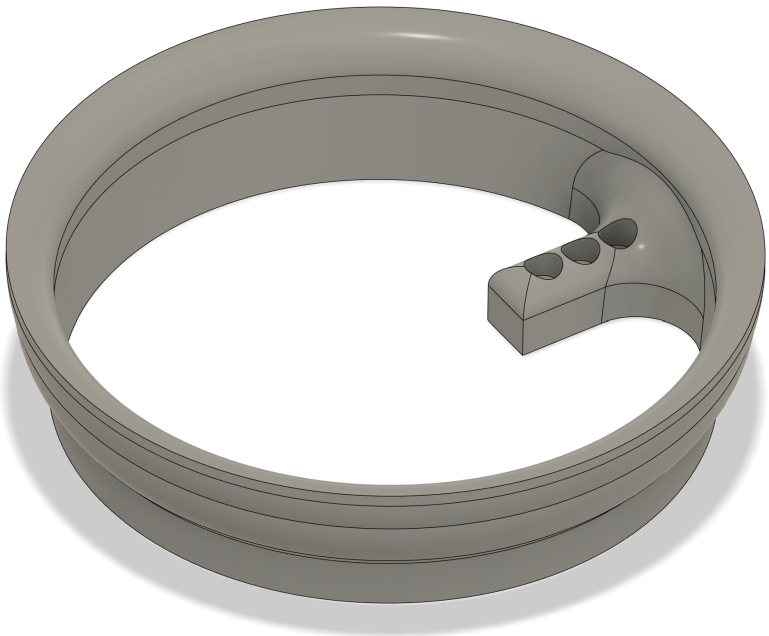

Figure 3.19: Duct–3D model

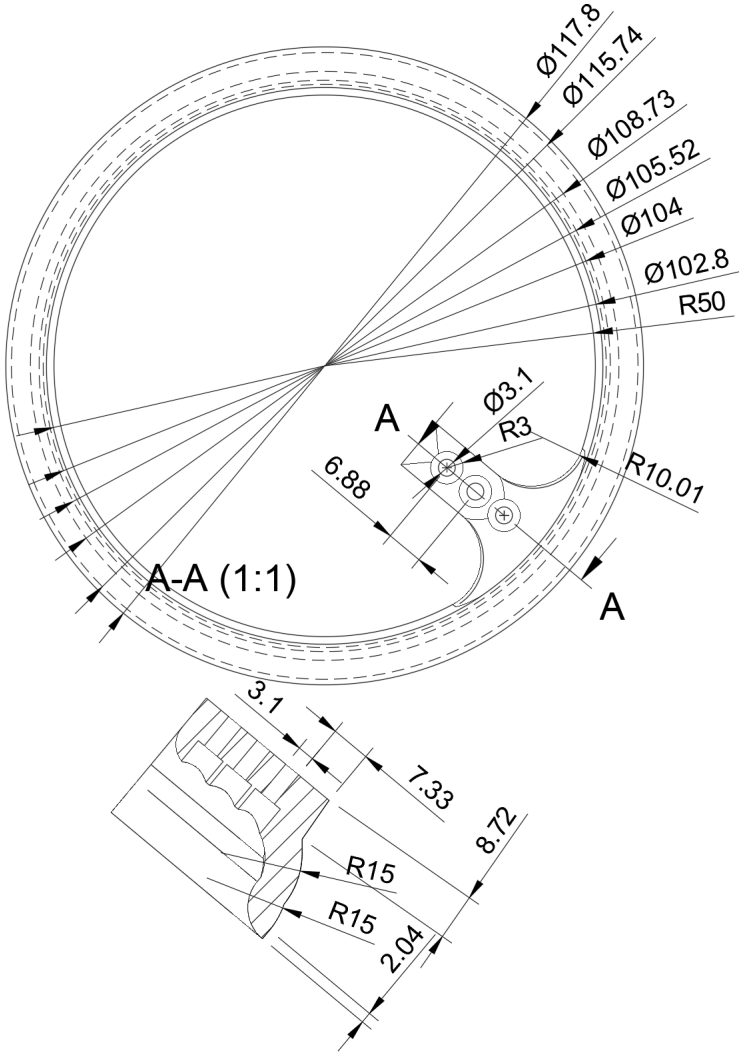

Figure 3.20: Duct–2D drawing

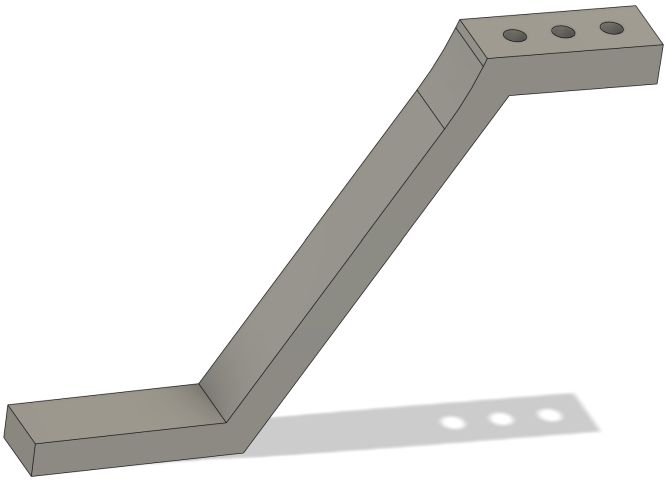

Figure 3.21: Gear–3D model

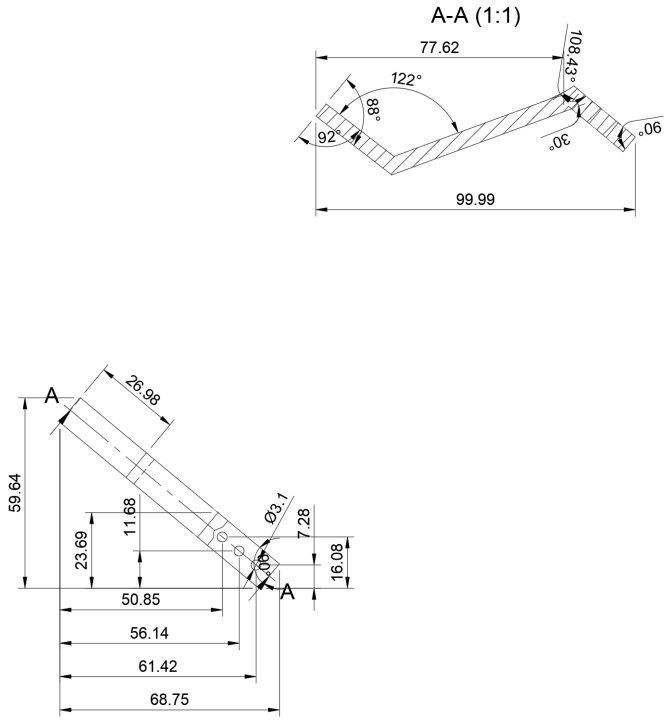

Figure 3.22: Gear–2D drawing

3.4 Power conversion design

The onboard power conversion subsystem in the tethered UAV architecture plays a critical role in ensuring stable and reliable power delivery to essential electronic components. To accommodate the varying voltage requirements of the onboard systems, two dedicated power conversion circuits were designed. The first circuit provides a regulated 5V output, primarily intended for the flight controller and the infrared-based lighthouse positioning system. The second circuit outputs 12V and is reserved for powering additional sensors or peripherals, thereby supporting potential future system expansions. Thus, the design flow is shown as the following:

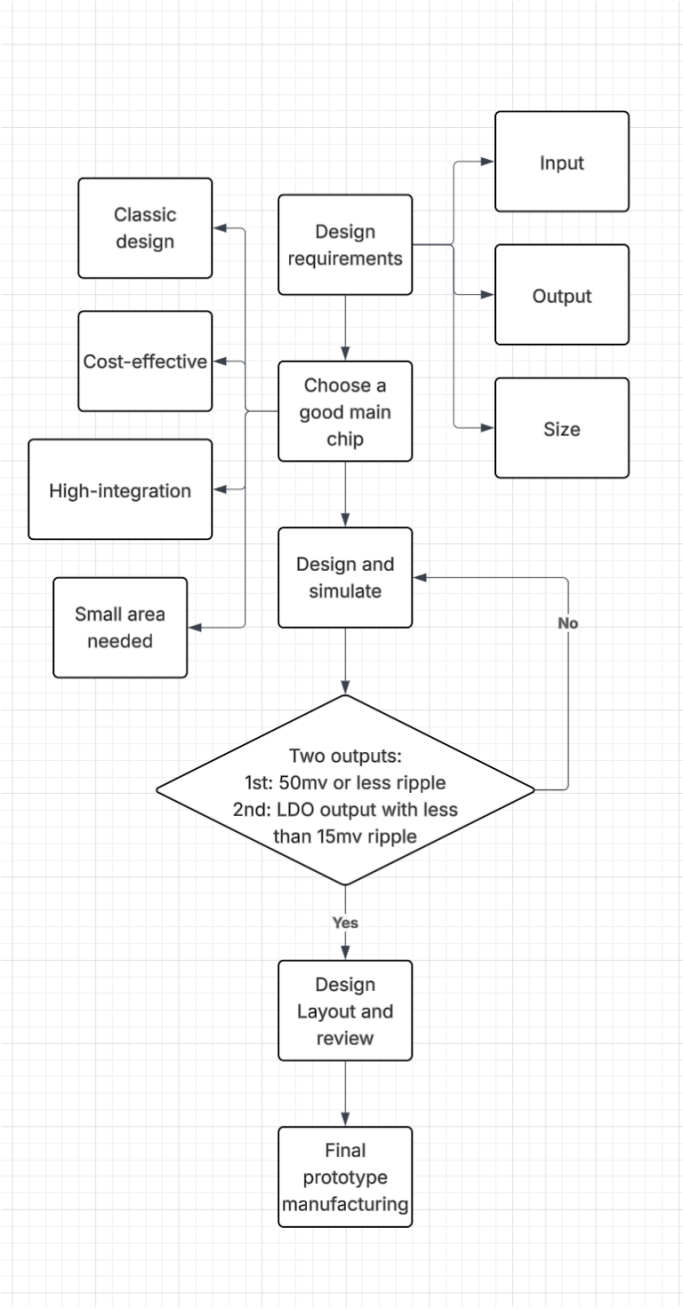

Figure 3.23: PCB design flow

3.4.1 5V output board

3.4.1.1 Requirements

1. Input:
   - Voltage Nominal: 24v
   - Voltage Range: 12v to 60v
   - Current: 3A maximum
2. Output:
   - Voltage: 5v
   - Maximum Current: 5A in total
   - LDO output: 2A maximum
3. Size:
   - Mounting points: 30.5mm x 30.5mm; M3
   - Area: $\leq$ 35mm x 35mm

3.4.1.2 PMIC selection

Based on the design considerations and power requirements outlined previously, the LM76005-Q1 was selected as the primary integrated circuit for voltage regulation. This device is a 5A synchronous step-down voltage regulator featuring integrated MOSFETs, which offers high efficiency, compact size, and robust performance. Its automotive-grade qualification and wide input voltage range make it well-suited for the stable power delivery required in the tethered UAV system.

3.4.1.3 Design and simulation

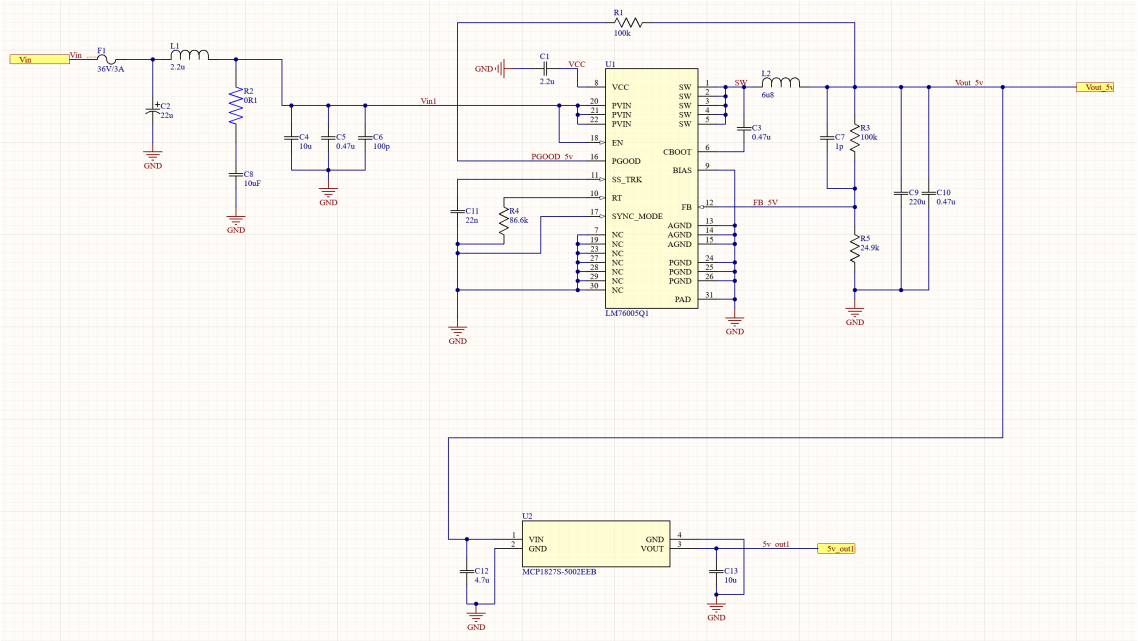

Figure 3.24: Schematic – 5v regulator module

The simulation was ran in PSPICE software for the main regulation part without the LDO part, as the rest should work well, and it will be known later after tests. Here is the simulation results:

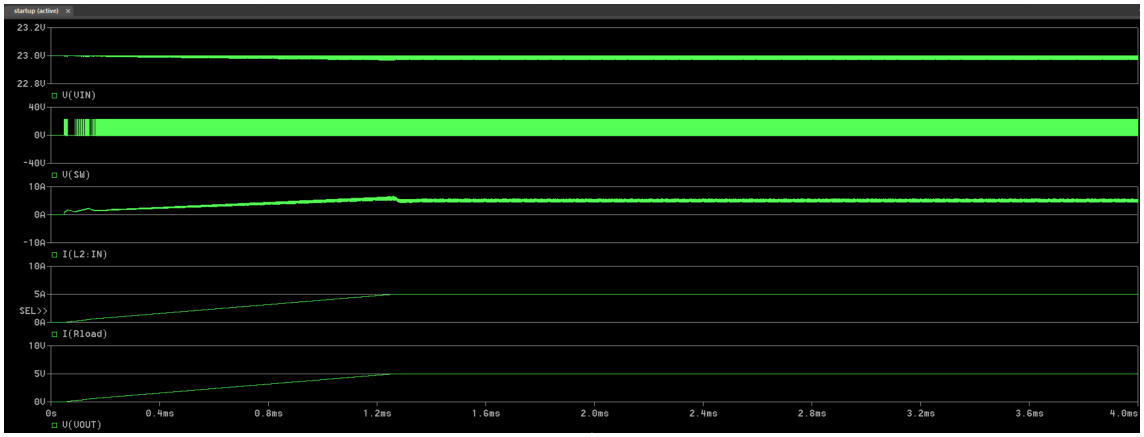

Figure 3.25: General simulation result – 5v regulator module

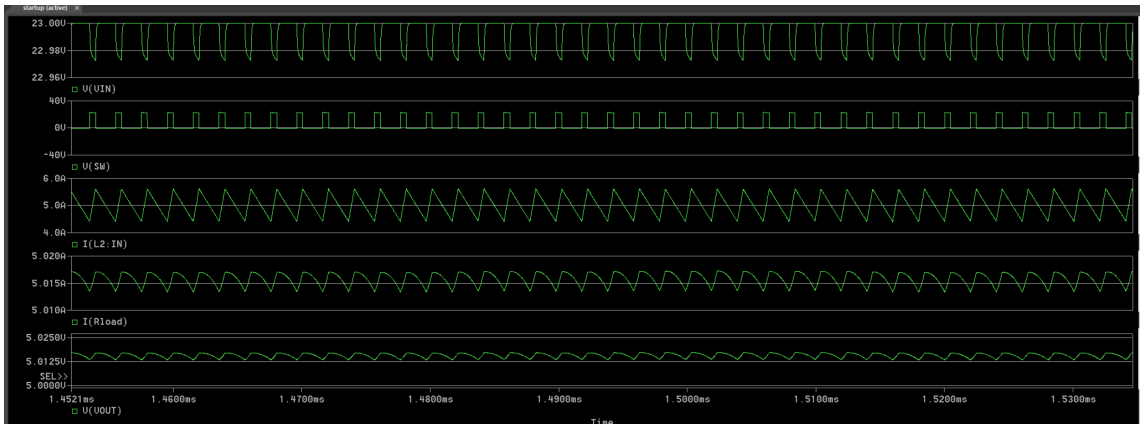

Figure 3.26: Detailed simulation result – 5v regulator module

The simulation is obvious that it satisfy the requirements, but in reality the output ripple could be bigger or smaller due to different reasons. The ripple is about 10mv at last with an input ripple of 1v. The input is set like this due to the reason that the input is actually an output from PDU which usually have a frequency of larger than 400khz with about 250mv ripple on the output side.

3.4.1.4 Board

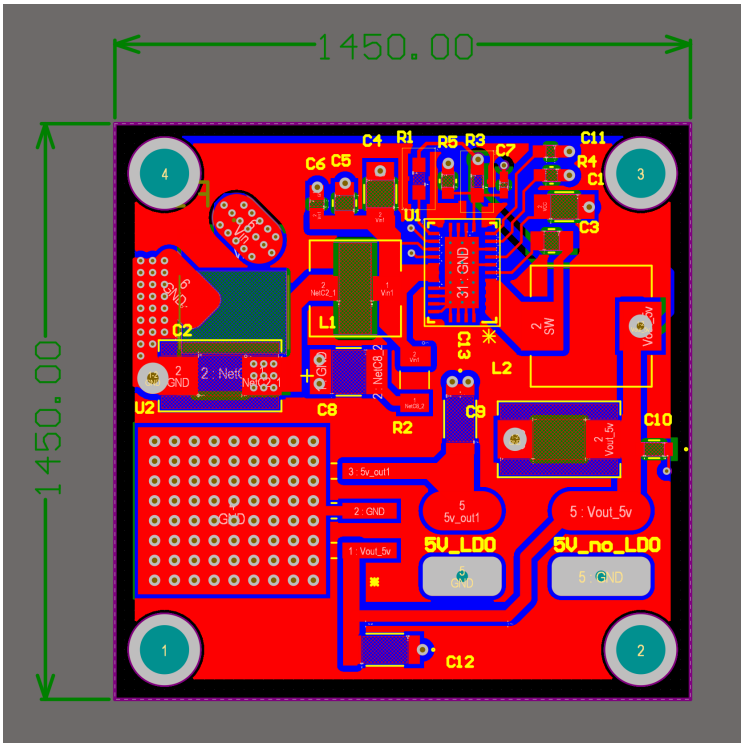

Figure 3.27: PCB1

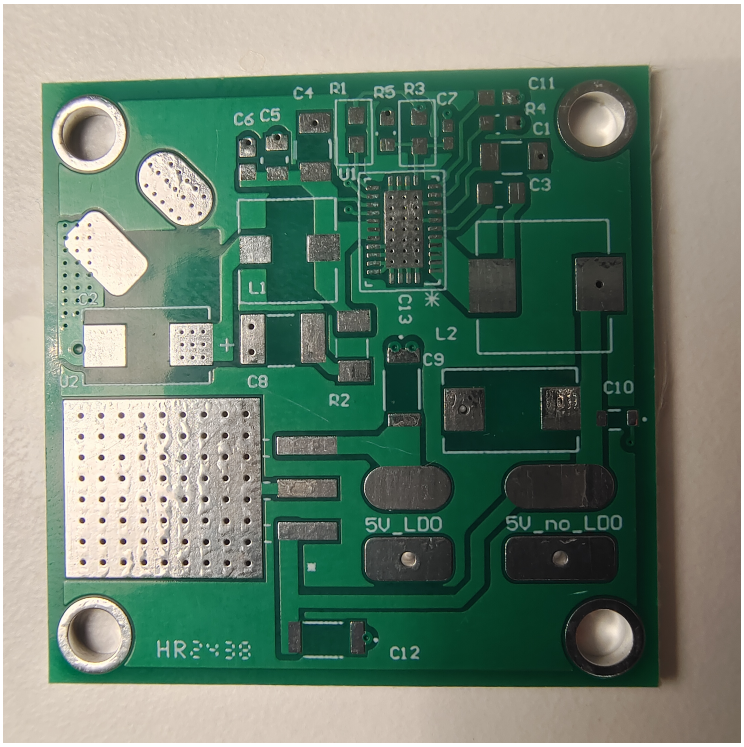

Figure 3.28: 5V regulation board

3.4.1.5 Circuit Test

- Input: PDU 24v output;
- Output voltage with no load: 5.12V ± 0.01V with 8mV of ripple;
- Output voltage with stable maximum load (4.5A ± 0.1A) (tested for 12 hours): 5.06V ± 0.02V with about 35mV ± 2V of ripple;
- Output voltage with maximum load (5.5A ± 0.1A) without LDO (can sustain maximum 17 seconds until automatical shutdown, can re-start): 5.04v ± 0.02v with 25mV of ripple;
- Ouput voltage with maximum load (1.5A ± 0.2A on the LDO side, 3.5A ± 0.2A on the common output side, can sustain about 30 seconds before automatically shutdown, can re-start): 4.97V ± 0.02V with 25mV ± 1mV of ripple and on the LDO output side; 5.01V ± 0.04V on the common output with 150mV ± 10mV;

3.4.1.6 Summary

After all, the LDO output is deleted because it seems not necessary after several long-term test. The LDO brought more ripples to the original output due to the inherited problems from the LDO IC's topology which affect the main frequency in bad way. Also, the fuse was changed to a smaller one, a 2A one in order to shutdown the circuit before the main IC fails.

3.4.2 12V output board

3.4.2.1 Requirements

1. Input:
   - Voltage Nominal: 24v
   - Voltage Range: 12v to 60v
   - Current: 3A maximum
2. Output:
   - Voltage: 12v
   - Maximum Current: 5A in total
   - LDO output: 1A maximum
3. Size:
   - Mounting points: 30.5mm x 30.5mm; M3
   - Area: $\leq$ 35mm x 35mm

3.4.2.2 PMIC selection

To shorten the period of development, the PMIC is chosen as the same as the previous one.

3.4.2.3 Design and simulation

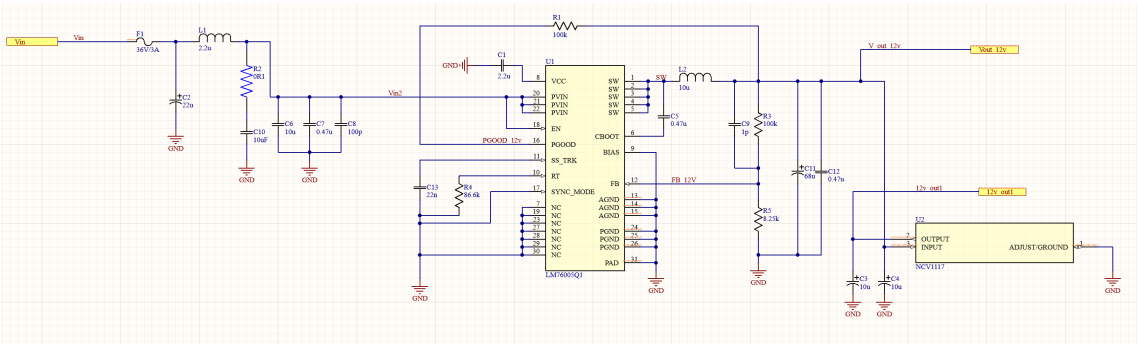

Figure 3.29: 12V board schematic

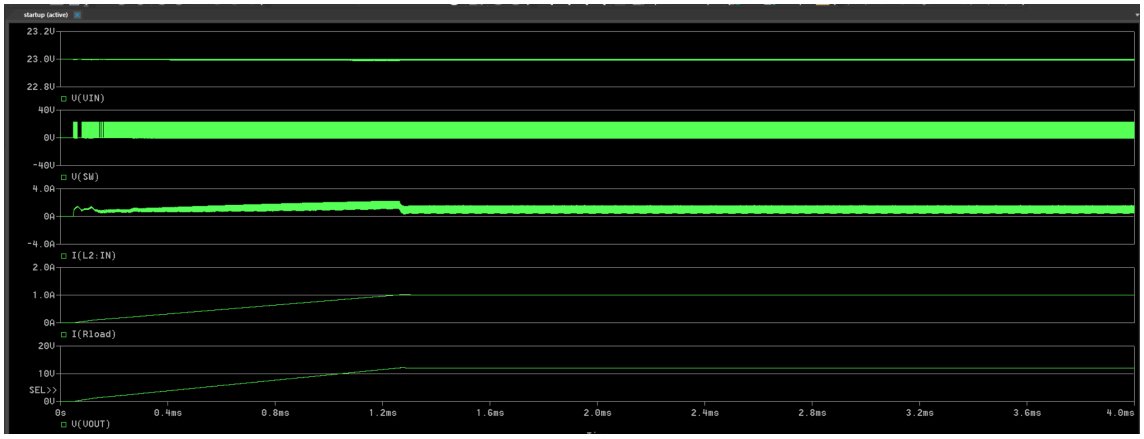

Figure 3.30: General simulation result – 12v regulator module

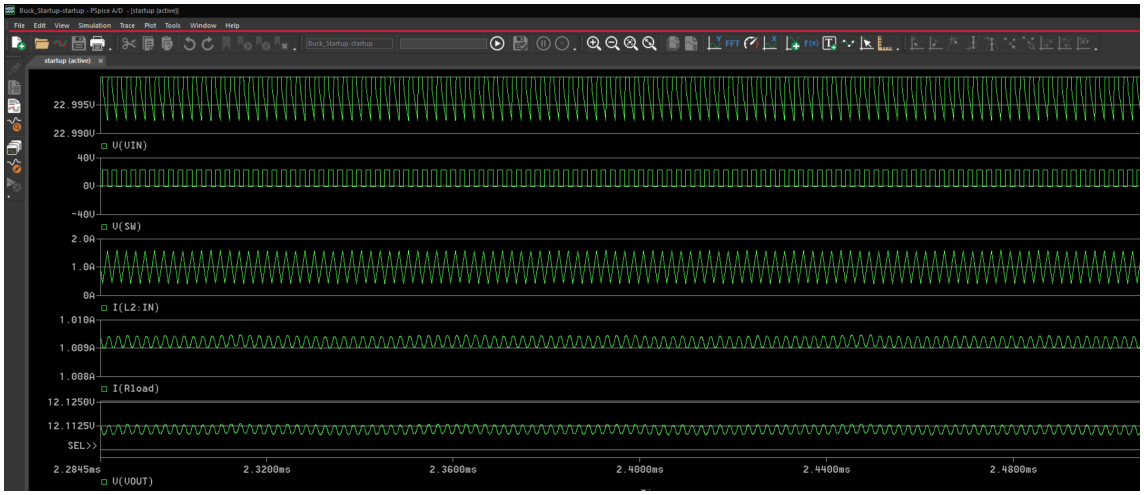

Figure 3.31: Detailed simulation result – 12v regulator module

The simulation obviously satisfy the requirements but certain changes may be made later after tests.

3.4.2.4 Board

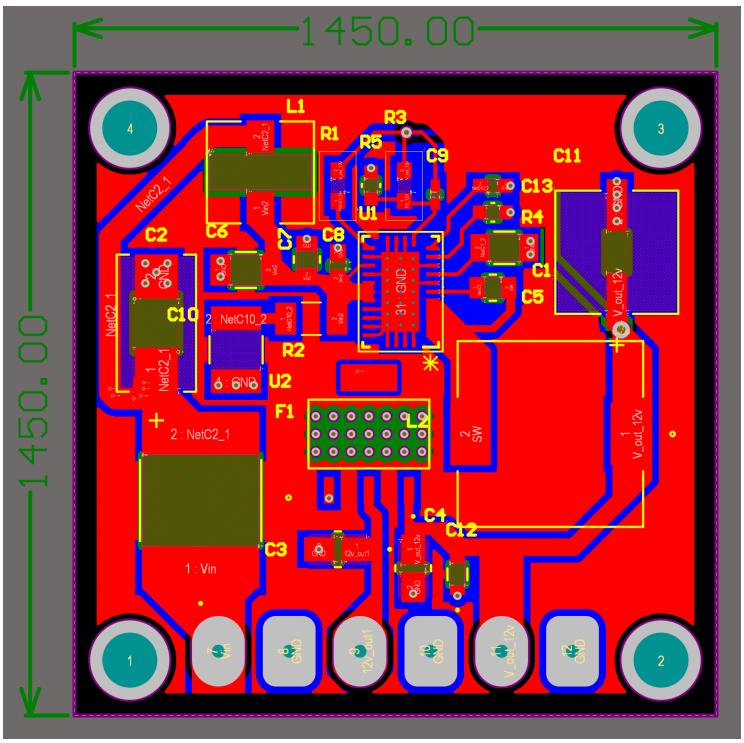

Figure 3.32: PCB1

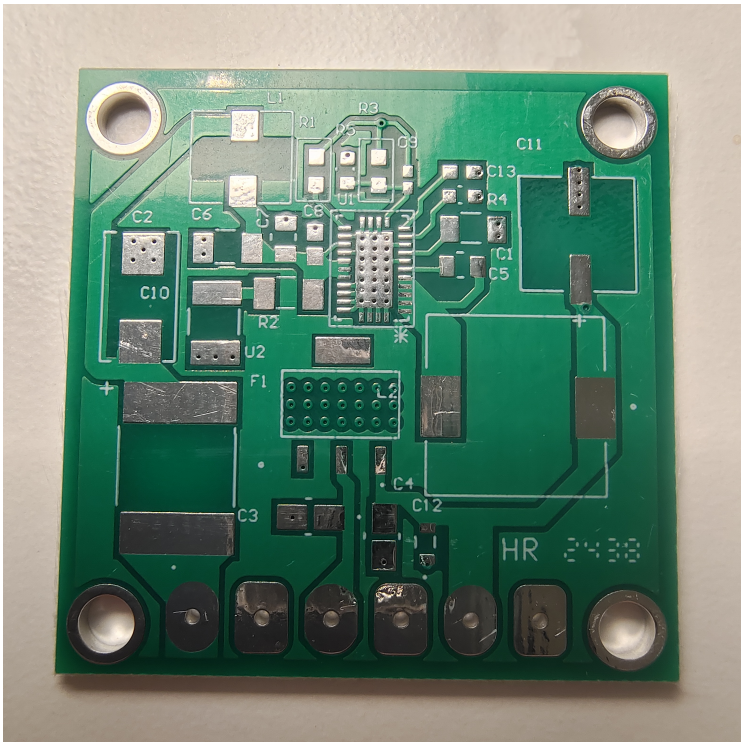

Figure 3.33: 5V regulation board

3.4.2.5 Circuit Test

- Input: PDU 24V output;
- Output voltage with no load: 12.13V ± 0.01V with 12mV of ripple;
- Output voltage with stable maximum load (4.7A ± 0.1A) (tested for 12 hours) without LDO output: 12.01V ± 0.02V with about 55mV ± 4mV of ripple;
- Output voltage with stable maximum load (3.3A ± 0.1A on the main output; 1A ± 0.1A on the LDO output side): 11.95V ± 0.01V with 5mV ± 1mV of ripple on the LDO output side; 12.02V ± 0.01V with 75mV ± 3mV on the common output side;
- Output voltage with maximum load (5.3A ± 0.1A) without LDO (can sustain 27 seconds until automatical shutdown, can re-start): 11.94V ± 0.03V with 115mV of ripple;
- Output voltage with maximum load (4.4A ± 0.1A on the common output side; 1.2A ± 0.05A on the LDO output side): can sustain 9 seconds, fuse burned, cannot re-start.

3.4.2.6 Summary

In summary, the LDO output is retained despite its minor influence on the main power output. This influence is minimal and does not significantly degrade performance, as the system continues to deliver a stable output with an acceptably low voltage ripple. Additionally, the fuse has been replaced with a 2.5A variant to ensure it activates prior to any automatic restart or sleep events caused by overcurrent or thermal protection mechanisms.

3.5 Final Assembly view

- Tethering drone No. 1:

Figure 3.34: Tethering Drone No. 1

Figure 3.35: Tethering Drone No. 2

Figure 3.36: Tethering system with tube connected

Two drones have been successfully assembled with fully functional systems, although one currently lacks two duct components due to damage sustained during crash testing. The third image depicts the fully assembled tethered drone, where a power and data cable is connected via a protective tube. This configuration is specifically designed for upcoming liquid transfer experiments, ensuring stable communication and power delivery while minimizing mechanical interference. The tethered setup also enhances operational safety and control during extended indoor testing scenarios.

3.6 Flight test and tuning

Flight testing and control tuning represent the most critical and time-intensive phases of the drone design process. These evaluations are conducted within a confined laboratory environment equipped with three infrared lighthouse base stations, which provide high-precision spatial tracking to facilitate accurate performance assessment and system calibration.

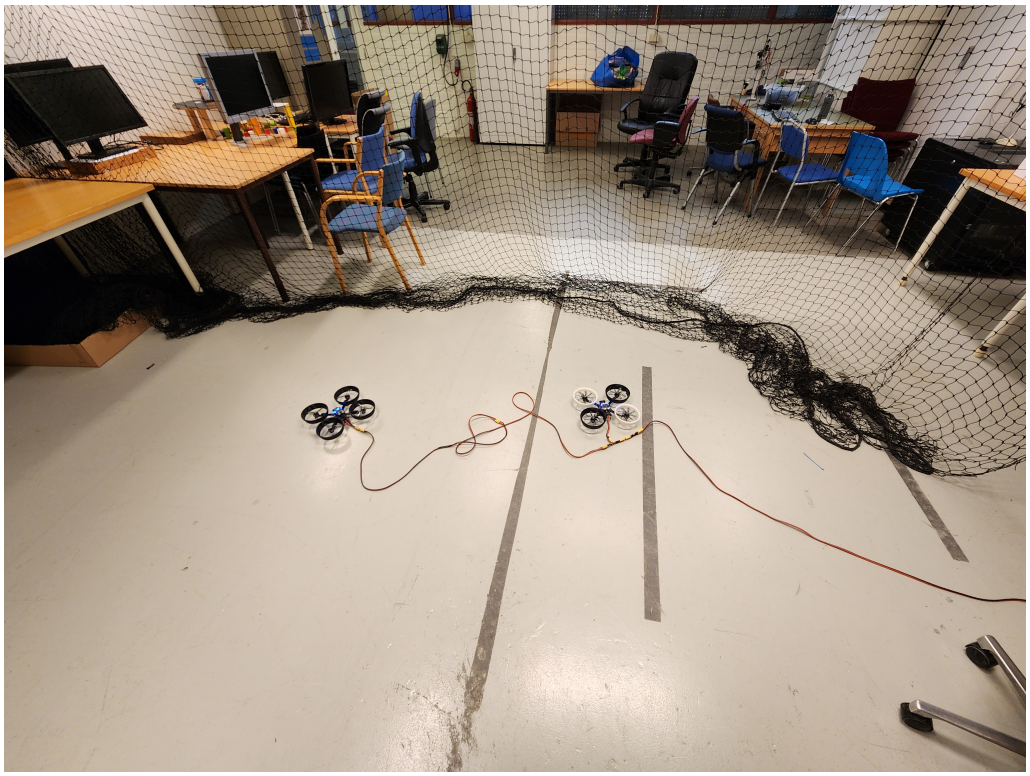

Figure 3.37: Testing environment

3.6.1 Environment Calibration

The first step to tune a precise indoor positioning system is to have a good calibration of it. The three base station is place in a way that they are compensate each other, as each of them covers a horizontal field of view of approximately 150 degrees and a vertical field of view of about 110 degree. And, according to the datasheet of the base station, it can have a range up to 10 meters, although during specific test, I discovered that it can maximum have an effective range to the drone at approximately 6 meters. Therefore, in a lab area of about 3m x 4m, those three base stations can be put like the following in order to get no dead area in the lab area.

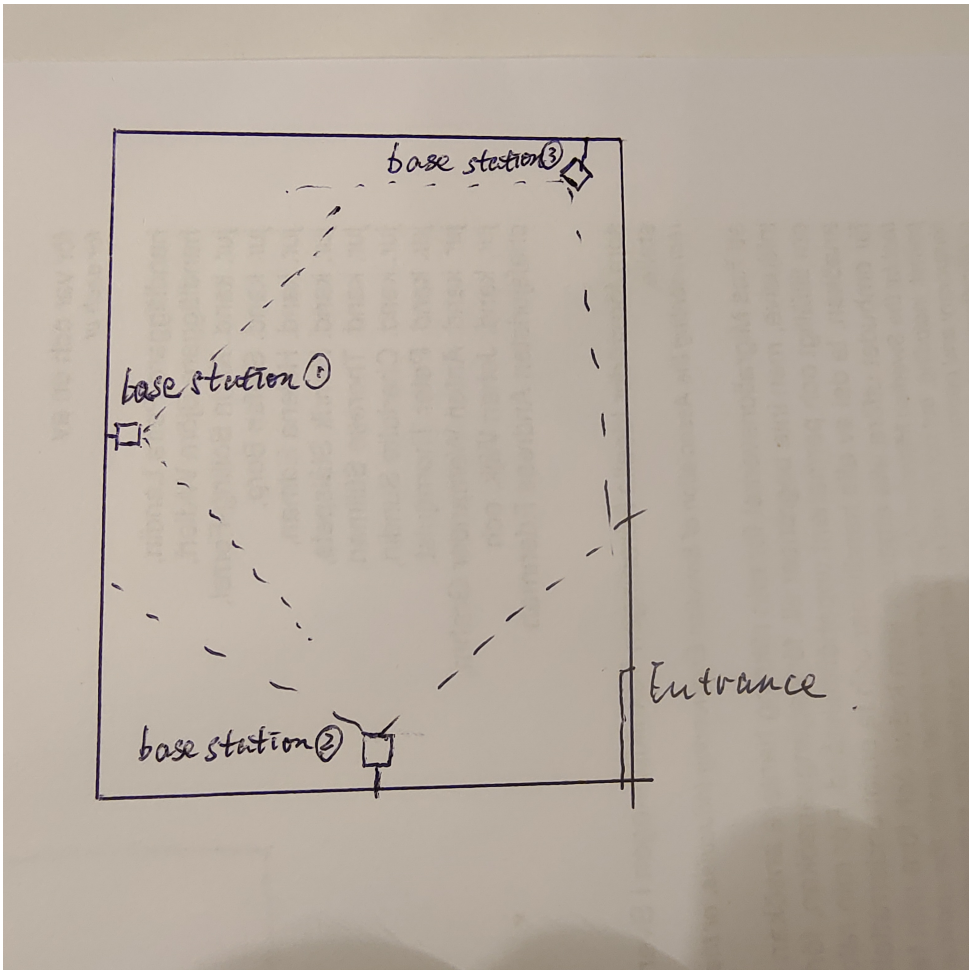

Figure 3.38: Base station positions

After the right placement of the base stations, the positioning deck installed on the UAV needs to be tested and calibrated, which will have a three-dimensional estimation of the lab area. Here is the result from the calibration:

Base station No.	X	Y	Z
1	1.05	0.22	2.98
2	-0.34	-2.94	2.97
3	-1.75	1.85	2.88

The estimation of the position of the base stations is quite reasonable, Therefore, further experiments can be started.

3.6.2 PID control loop

By default, the Crazyflie firmware implements a cascaded control architecture based on proportional-integral-derivative (PID) regulators to govern the drone's dynamic behavior. This architecture comprises a hierarchy of PID controllers, each responsible for a specific control domain: position, velocity, attitude, and angular rate. The

output of each higher-level controller serves as the reference input for the subsequent lower-level controller, thereby enabling precise and stable flight through a structured cascade of feedback loops [27].

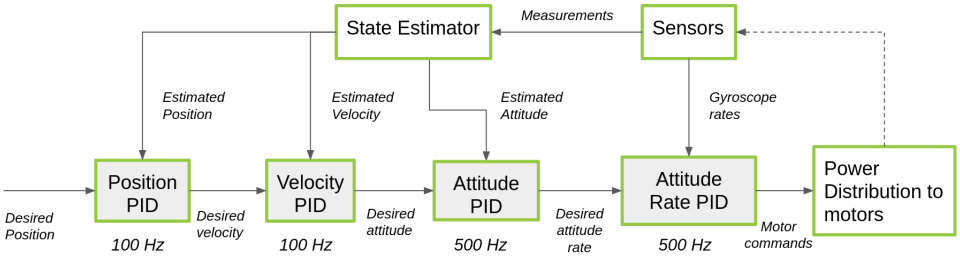

Figure 3.39: PID control of crazyflie firmware

Each loop computes control commands based on the error between desired setpoints and estimated states, with the output of each higher-level controller serving as the input for the subsequent lower-level controller.

- **Position Control**
  The position controller computes the desired velocity $\mathbf{v}_{\text{set}}$ based on the error between the desired position $\mathbf{p}_{\text{set}}$ and the estimated position $\mathbf{p}_{\text{est}}$:

$$\mathbf{v}_{\text{set}} = K_p^{\text{pos}}(\mathbf{p}_{\text{set}} - \mathbf{p}_{\text{est}}) + K_i^{\text{pos}} \int (\mathbf{p}_{\text{set}} - \mathbf{p}_{\text{est}})dt + K_d^{\text{pos}} \frac{d}{dt}(\mathbf{p}_{\text{set}} - \mathbf{p}_{\text{est}}) \quad (3.3)$$

- **Velocity Control**
  The velocity controller determines the desired attitude angles $\boldsymbol{\theta}_{\text{set}}$ using the velocity error:

$$\boldsymbol{\theta}_{\text{set}} = K_p^{\text{vel}}(\mathbf{v}_{\text{set}} - \mathbf{v}_{\text{est}}) + K_i^{\text{vel}} \int (\mathbf{v}_{\text{set}} - \mathbf{v}_{\text{est}})dt + K_d^{\text{vel}} \frac{d}{dt}(\mathbf{v}_{\text{set}} - \mathbf{v}_{\text{est}}) \quad (3.4)$$

- **Attitude Control**
  This controller computes the desired angular rate $\boldsymbol{\omega}_{\text{set}}$ based on the attitude error:

$$\boldsymbol{\omega}_{\text{set}} = K_p^{\text{att}}(\boldsymbol{\theta}_{\text{set}} - \boldsymbol{\theta}_{\text{est}}) + K_i^{\text{att}} \int (\boldsymbol{\theta}_{\text{set}} - \boldsymbol{\theta}_{\text{est}})dt + K_d^{\text{att}} \frac{d}{dt}(\boldsymbol{\theta}_{\text{set}} - \boldsymbol{\theta}_{\text{est}}) \quad (3.5)$$

- **Angular Rate Control**
  The final control loop calculates the control signal $\mathbf{u}$ (typically converted to PWM signals) to drive the motors:

$$\mathbf{u} = K_p^{\text{rate}}(\boldsymbol{\omega}_{\text{set}} - \boldsymbol{\omega}_{\text{est}}) + K_i^{\text{rate}} \int (\boldsymbol{\omega}_{\text{set}} - \boldsymbol{\omega}_{\text{est}})dt + K_d^{\text{rate}} \frac{d}{dt}(\boldsymbol{\omega}_{\text{set}} - \boldsymbol{\omega}_{\text{est}}) \quad (3.6)$$

In summary, those controller enables the drone to possibly have a good flying pattern in a dynamic environment, but certain tuning process is needed.

3.6.3 Flight Tests

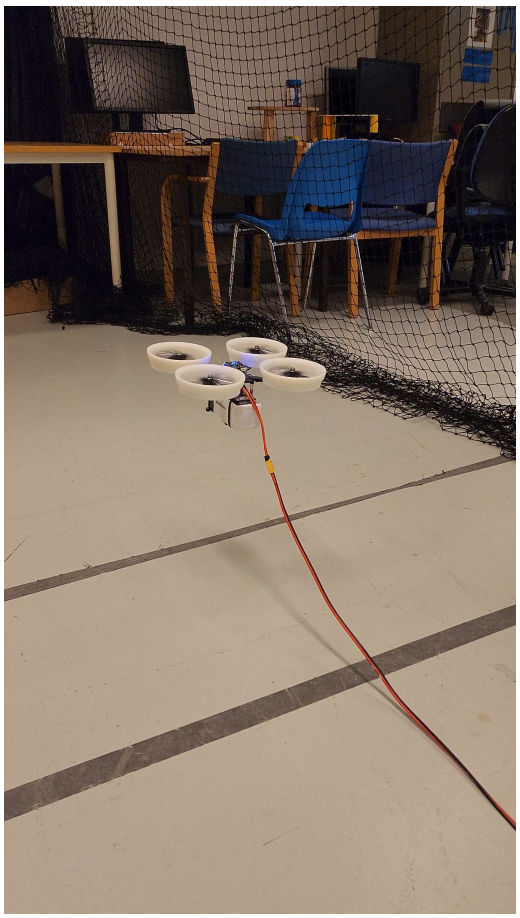

Figure 3.40: Flight test with payload

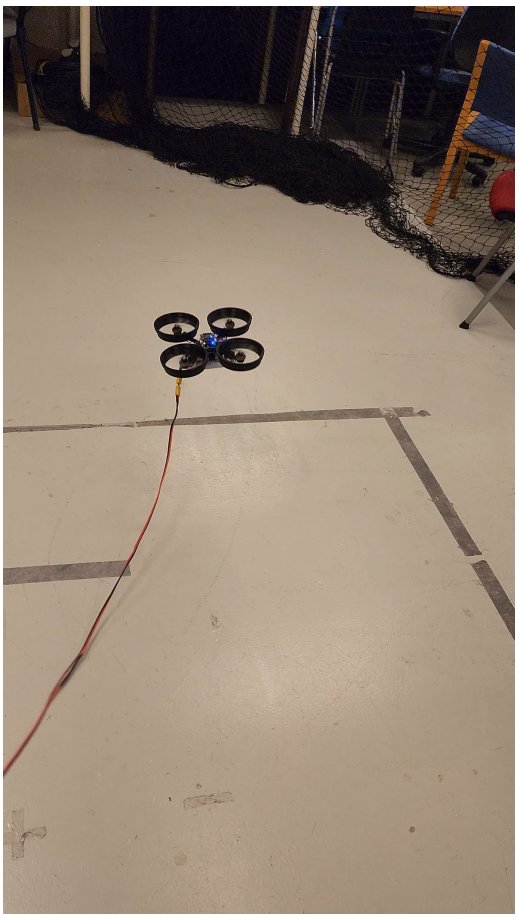

Figure 3.41: Flight test without payload

The primary objective of the manual flight tests was to fine-tune the UAV's flight characteristics to achieve a response that aligns intuitively with pilot inputs—a process often described as enabling the drone to "follow the hand." This subjective measure of controllability serves as an initial reference for tuning the flight control loop. The flight controller used in this project, based on the Bitcraze Crazyflie 2.1 architecture, utilizes a cascaded PID control structure. In this configuration, outer-loop attitude controllers compute desired angular velocities, which are then passed to inner-loop rate controllers. Each axis (roll, pitch, yaw) is governed by a proportional–integral–derivative (PID) controller, with gains empirically tuned to optimize responsiveness and stability. The control mode was initially set to "angle" mode but was quickly switched to "rate" mode (also known as "ACRO" mode), disabling auto-leveling and enabling more precise tuning of angular rate response based on the pilot's perception of agility and damping.

Tuning was conducted over multiple test flights, relying on empirical adjustments due to the absence of a physics-based simulation environment for this custom, tethered system. The gains were iteratively adjusted to minimize overshoot, reduce

oscillations, and ensure responsive but stable maneuvering. For instance, increasing the derivative term on the pitch axis helped dampen fast oscillations during aggressive forward tilts, while moderate integral gains on roll ensured stability against drift without introducing windup effects. Such tuning is very customized to the ESC and the motors' current performance, it might requires changes for a different drone with the same size.

The original PID values are shown as the following:

Controller	Type	P	I	D	FF(Feed-Forward gain)
Rate	Roll	500	500	5	No FF option
	Pitch	500	500	5	
	Yaw	100	50	5	
Attitude	Roll	5	5	5	No FF option
	Pitch	5	5	5	
	Yaw	5	5	5	
Velocity	X	25	25	5	5
	Y	25	25	5	5
	Z	25	25	5	No FF option
Position Control	X	5	5	5	No FF option
	Y	5	5	5	
	Z	5	5	5	
Hover Thrust	32768				

After many iterations of tuning, I got the following:

Controller	Type	P	I	D	FF(Feed-Forward gain)
Rate	Roll	150	100	3	No FF option
	Pitch	150	100	3	
	Yaw	50	15	1.5	
Attitude	Roll	4	1.2	1.1	No FF option
	Pitch	4	1.2	1.1	
	Yaw	2	0.7	0.25	
Velocity	X	15	8	6	2.5
	Y	15	8	6	2.5
	Z	12	7	3	No FF option
Position Control	X	5	5	5	No FF option
	Y	5	5	5	
	Z	5	5	5	
Hover Thrust	2000				

A major technical challenge was scaling the control system from the original 50g Crazyflie micro-UAV to a significantly larger and heavier tethered prototype (800

g), equipped with high-thrust brushless motors and larger propellers. This 16-fold increase in mass required not only recalibration of control parameters but also reevaluation of the component endurance under real-world conditions. Motor selection was particularly critical; two candidate motors failed during testing—likely due to thermal overload or sustained high torque at low throttle conditions. Similarly, four ESCs were damaged, with root causes including overcurrent during locked-rotor scenarios and possible signal integrity issues between the flight controller and ESC pulse-width modulation (PWM) interface.

After many iterations, the AMAX 2005 brushless motor and SpeedyBee 55A BLHeli-32 ESC combination proved to be the most reliable. The ESC, rated for a burst current of 75 A and continuous 55 A, showed resilience under dynamic loads. Thermal monitoring confirmed that the selected ESC remained within safe operating limits during aggressive flight maneuvers, suggesting effective power delivery and MOSFET cooling design. This combination formed a robust foundation for further testing and long-term operation within the tethered UAV system. While a detailed root-cause analysis of failed components was not feasible due to project constraints, the empirical approach adopted here successfully identified a viable and durable propulsion configuration for indoor tethered flight operations.

3.6.4 Automatic control tuning

The process of automatic flight control tuning proved to be both time-consuming and technically demanding throughout the course of this project. This complexity may stem from several contributing factors, including the prototype nature of the UAV platform and the inherent difficulty in achieving a well-balanced control response across multiple axes. The absence of a high-fidelity simulation environment also meant that tuning had to be performed entirely through real-world flight tests, further increasing the time and resources required. Nevertheless, through systematic experimentation and empirical tuning, a relatively stable configuration was eventually achieved, enabling the UAV to maintain autonomous hover and basic maneuvering with acceptable precision.

The original maneuvering, with default PID values looks looks like the following:

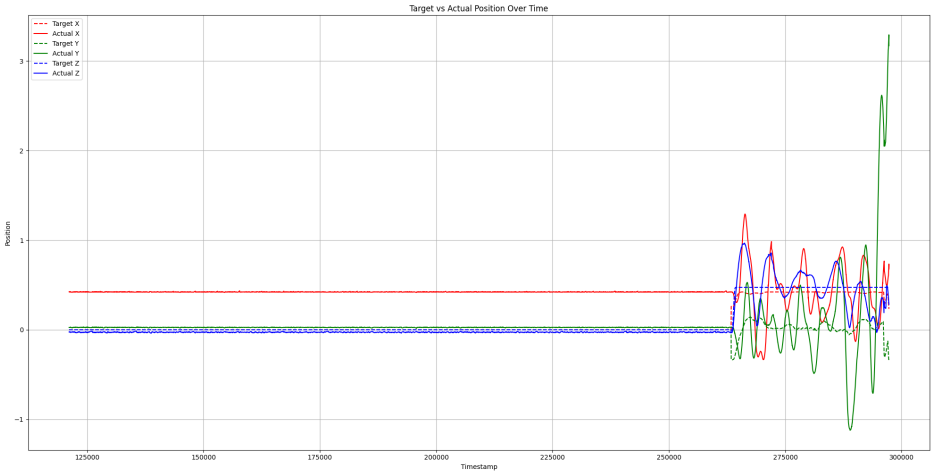

Figure 3.42: One of the single drone tests plot in 2D

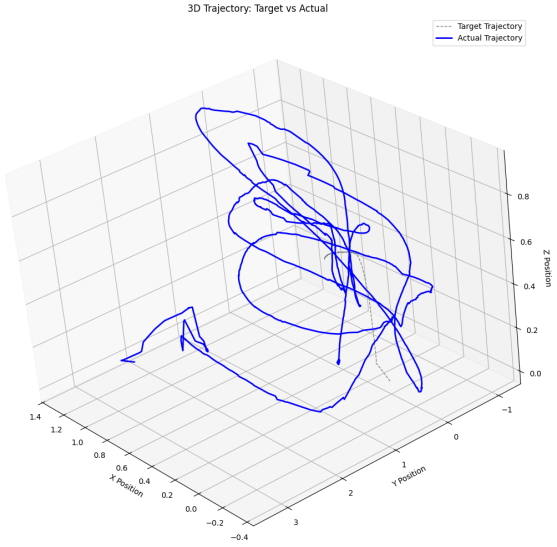

Figure 3.43: One of the single drone tests plot in 3D

It is obvious that there are lots of combined problems such as PID overshooting, actuator saturation, and so on. During the test different kinds of values have been tried but the progress is little in the final output. Nevertheless, after weeks of tuning, the single tethered drone can successfully flying in an acceptable stability although the position PID values are still need more fine tuning. The tuned PID values are shown below:

Controller	Type	P	I	D	FF(Feed-Forward gain)
Rate	Roll	150	100	8	No FF option
	Pitch	150	100	8	
	Yaw	50	15	4	
Attitude	Roll	4	2.5	1.7	No FF option
	Pitch	4	2.5	1.7	
	Yaw	2	0.7	0.25	
Velocity	X	21	12	7	4
	Y	21	14	5	2.5
	Z	12	7	3	No FF option
Position Control	X	5	2.3	1.5	No FF option
	Y	5	2.3	1.5	
	Z	3	2	1.5	
Hover Thrust	2500				

The flying pattern is shown as the below:

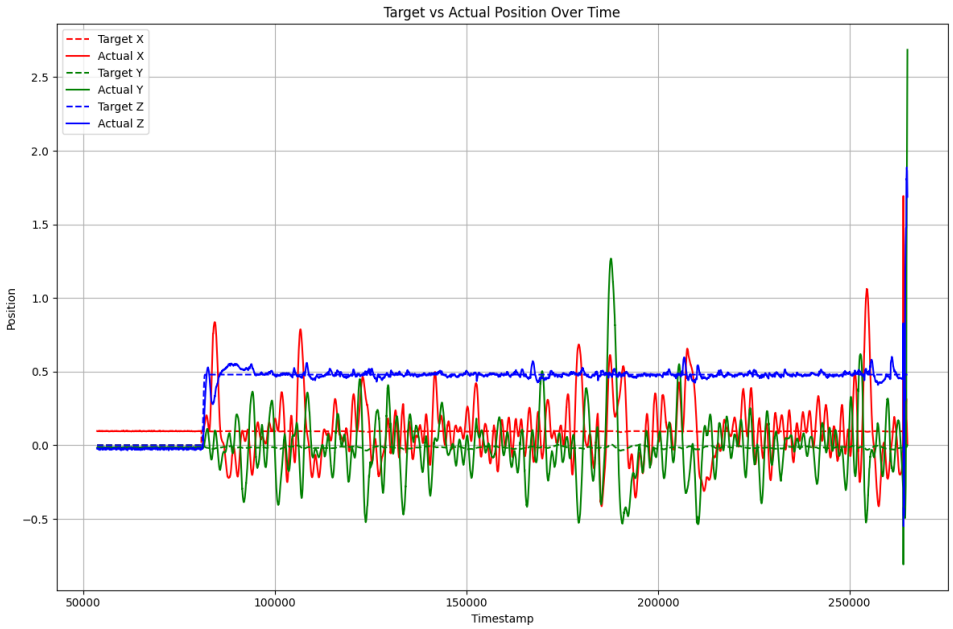

Figure 3.44: One of the final single drone tests plot in 2D

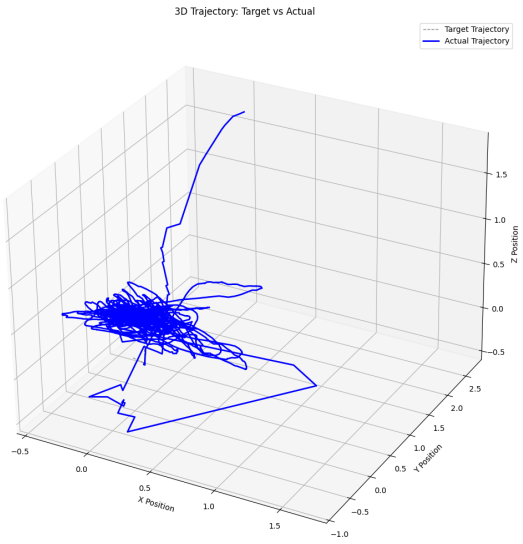

Figure 3.45: One of the final single drone tests plot in 3D

The above plots illustrate the UAV's performance during autonomous flight with PID control. The 3D trajectory plot shows a significant deviation between the target and actual paths, particularly at the beginning, indicating instability and high-frequency oscillations—likely due to aggressive proportional or insufficient derivative gains. The 2D position-over-time plot reveals that altitude control (Z-axis) is relatively stable with minimal error after initial transients, suggesting effective vertical PID tuning. In contrast, lateral motion (X and Y axes) exhibits persistent oscillations and overshooting, highlighting tuning imbalances, possible signal noise, or dynamic coupling effects such as tether interference. Overall, while the vertical control loop is well-tuned, the horizontal position control requires further optimization, possibly through reduced P gain, increased D gain, and the addition of filtering or adaptive tuning strategies.

4
Conclusions

4.1 Conclusions

This project successfully established a functional indoor tethering system integrated with a precise optical-based positioning infrastructure, tailored for indoor multi-UAV applications. Although the current implementation supports only a single drone, the system architecture was deliberately designed for scalability, and extending it to accommodate additional UAVs requires only minor material augmentations without substantial modifications to the core infrastructure. In parallel, a customized UAV platform was developed, incorporating a robust onboard power supply and distribution circuit. The structural design of the drone, alongside the reliability of the onboard electronics, played a crucial role in ensuring stable and safe operation under tethered power. Furthermore, a fundamental control loop was successfully tuned to achieve a relatively stable flight performance. While the current positioning control still exhibits room for improvement in terms of precision, the results demonstrate a solid foundation for further refinement. With continued development, the control accuracy and system resilience are expected to improve, supporting broader deployment in indoor robotic applications.

4.2 Discussion

The developed tethering system, with its stable indoor positioning, continuous power supply, and modular design, opens a wide array of application possibilities beyond simple UAV operation. Its long-term operational capability, safety-focused design, and ability to support high-power consumption make it particularly suited for industrial, laboratory, and inspection environments where traditional battery-powered drones are limited by flight time and operational stability.

- **Robotic manipulation for Manufacturing Environments:**
  The tethered UAV system can be adapted as a free-moving robotic manipulator in advanced manufacturing processes, effectively acting as a robotic "hand" or mobile tool carrier. For example, in a car assembly line, such a system can carry tools or sensors to hard-to-reach areas of a vehicle's chassis, performing tasks like spot welding, component inspection, or even real-time calibration. Unlike fixed-arm robots, the tethered UAV offers flexible reach within a large workspace, while the power tether ensures uninterrupted operation and high payload capacity.
- **Liquid Transfer and Sampling in Chemical Laboratories:**

In sensitive chemical laboratory environments, where human interaction may be hazardous or contamination-prone, a tethered UAV can be employed to perform tasks such as liquid sampling, transfer between stations, or mixing operations. The UAV's capacity for precise localization and extended operational time makes it suitable for tasks requiring careful handling. For instance, in a bio-lab, it could transfer microfluidic samples between PCR machines and imaging stations without requiring physical transport by personnel, thus reducing risk and improving throughput.

- **Long-term surveillance and monitoring:**
  The tethering system is inherently advantageous for persistent surveillance and environmental monitoring tasks. With its unlimited power supply and stable indoor or semi-outdoor flight, it can remain airborne for extended periods—hours or even days—unlike conventional drones. Applications include monitoring security-sensitive zones such as data centers, airports, or museums. Additionally, in scenarios such as underground infrastructure or warehouse automation, the tethered UAV can provide persistent visual or sensor-based feedback without interruption.
- **Structural Inspection for Aircraft and Civil Infrastructure:**
  The tethering system is inherently advantageous for persistent surveillance and environmental monitoring tasks. With its unlimited power supply and stable indoor or semi-outdoor flight, it can remain airborne for extended periods—hours or even days—unlike conventional drones. Applications include monitoring security-sensitive zones such as data centers, airports, or museums. Additionally, in scenarios such as underground infrastructure or warehouse automation, the tethered UAV can provide persistent visual or sensor-based feedback without interruption.
- **Marine Applications and Remote Sensor Deployment:**
  Beyond terrestrial use, the tethering system can be mounted on vessels to enable sensor deployment in marine environments. A drone, powered via tether from a ship, could carry sensors to specific locations in the sea for water quality monitoring, sonar scanning, or equipment placement. This approach could eliminate the need for robotic arms or divers in certain use cases. The modular nature of the UAV also allows it to return, swap tools, and redeploy with different sensors or payloads as needed.

In essence, the tethering system designed in this project has demonstrated not only immediate applicability for UAV power and positioning, but also broader relevance across multiple industries. Its scalable architecture, continuous power delivery, and flexible deployment capabilities position it as a promising platform for a new class of long-duration, semi-autonomous aerial robots in both structured and semi-structured environments.

Bibliography

[1] Brennan torpedo. (2015, June 1). In Wikipedia. *https://en.wikipedia.org/wiki/Brennan_torpedo*

[2] Fan, S., Chan, K., and Chin, C. K. (2020). Motion analysis of an autonomous underwater vehicle tethered with an optical fiber for real-time surveillance. *IEEE Journal of Oceanic Engineering, 46(2):434–446.*

[3] Bowen, A., German, C., Jakuba, M., Kinsey, J. C., Mayer, L., Yoerger, D., and Whitcomb, L. L. (2012). Lightly tethered unmanned underwater vehicle for under-ice exploration. *In 2012 IEEE Aerospace Conference, pages 1–12. IEEE.*

[4] Santos, J. S., Stevanovic, S., Kondak, K., Holzapfel, F., Góes, L. C., and Pant, R. S. (2016). Stability augmentation system for a tethered airship. In *16th AIAA Aviation Technology, Integration, and Operations Conference, page 4224.*

[5] Kiribayashi, S., Ashizawa, J., and Nagatani, K. (2015). Modeling and design of tether powered multicopter. In *2015 IEEE International Symposium on Safety, Security, and Rescue Robotics (SSRR), pages 1–7. IEEE.*

[6] Gu, B. W., Choi, S. Y., Choi, Y. S., Cai, G., Seneviratne, L., and Rim, C. T. (2016). Novel roaming and stationary tethered aerial robots for continuous mobile missions in nuclear power plants. *Nuclear Engineering and Technology, 48(4):982–996.*

[7] Walendziuk, W., Oldziej, D., and Slowik, M. (2020). Power supply system analysis for tethered drones application. In *2020 International Conference Mechatronic Systems and Materials (MSM)*, pages 1–6. IEEE.

[8] Li, Y.-b. andWang, X. (2011). Ground station software design of tethered airship monitoring system. In *2011 International Symposium on Computer Science and Society, pages 332–335. IEEE.*

[9] Chandrasekharan, S., Gomez, K., Al-Hourani, A., Kandeepan, S., Rasheed, T., Goratti, L.,Reynaud, L., Grace, D., Bucaille, I.,Wirth, T., et al. (2016). Designing and implementing future aerial communication networks. **IEEE Communications Magazine, 54(5):26–34.**

[10] Huthaifa Ahmad Obeidat, Wafa Shuaieb, Omar Obeidat and Raed AbdAlhameed, A Review of Indoor Localization Techniques and Wireless Technologies, *Wireless Personal Communications, vol. 119, pp. 289-327, 2021.*

[11] Kyle Wroble, Performance Analysis of Magnetic Indoor Local Positioining System, *Western Michigan University, 2017.*

[12] Priyantha, N. B., Chakraborty, A., Balakrishnan, H. (2000). The Cricket location-support system. *Proceedings of the 6th Annual International Conference on Mobile Computing and Networking (MobiCom), 32–43.*

[13] Liu, H., Darabi, H., Banerjee, P., Liu, J. (2007). Survey of wireless indoor positioning techniques and systems. *IEEE Transactions on Systems, Man, and Cybernetics, Part C (Applications and Reviews), 37(6), 1067–1080.*

[14] Sonntag, R., Wills, L. M. (2004). Underwater acoustic positioning systems. *Sea Technology, 45(9), 17–22.*

[15] Damir Arbula and Sandi Ljubic, Indoor Localization Based on Infrared Angle of Arrival Sensor Network, *Sensors MDPI, vol. 20, no. 21, p. 6278, 2020.*

[16] Yassin, M., Nasser, Y., Awad, M., Al-Dubai, A., Liu, R., Umer, T. (2017). Recent advances in indoor localization: A survey on theoretical approaches and applications. *IEEE Communications Surveys Tutorials, 19(2), 1327–1346.* https://doi.org/10.1109/COMST.2016.2632427

[17] Gu, Y., Lo, A., Niemegeers, I. (2009). A survey of indoor positioning systems for wireless personal networks. *IEEE Communications Surveys Tutorials, 11(1), 13–32.* https://doi.org/10.1109/SURV.2009.090103

[18] Alavi, B., Pahlavan, K. (2006). Modeling of the TOA-based distance measurement error using UWB indoor radio measurements. *IEEE Communications Letters, 10(4), 275–277.* https://doi.org/10.1109/LCOMM.2006.1618945

[19] Tiemann, J., Schweikowski, F., Wietfeld, C. (2017). Design of an UWB indoor-positioning system for UAV navigation in GNSS-denied environments. *IEEE International Conference on Indoor Positioning and Indoor Navigation (IPIN), 1–7.* https://doi.org/10.1109/IPIN.2015.7346766

[20] Luca Mainetti, Luigi Patrono, and Ilaria Sergi, "A Survey on Indoor Positioning Systems," *2014 22nd International Conference on Software, Telecommunications and Computer Networks (SoftCOM), pp. 111-120, 2015.*

[21] Bitcraze AB. (2021). Lighthouse Positioning System. *https://www.bitcraze.io/documentation/system/lighthouse/*

[22] Hartley, R., Zisserman, A. (2004). *Multiple View Geometry in Computer Vision (2nd ed.). Cambridge University Press.*

[23] Ghassemi, H., Zangeneh, M. (2007). Ducted propeller design and analysis in non-uniform wake field. *Scientia Iranica, 14(4), 323–330.*

[24] Tognaccini, R., Ballerini, G., Sannino, R. (2019). Design of ducted propellers. *NuTTS 2019*

[25] Saeed, A., Kim, D. (2015). Performance of a ducted propeller designed for UAV applications at hover and forward flight. *Aerospace Science and Technology, 45, 174–182.*

[26] Lind, A. H., Smith, B. T. (2012). Experimental investigation of a ducted propeller. *European Conference for AeroSpace Sciences (EUCASS).*

[27] Bitcraze. Crazyflie Firmware Documentation. *[Online]. Available: https://github.com/bitcraze/crazyflie-firmware*

DEPARTMENT OF SOME SUBJECT OR TECHNOLOGY
CHALMERS UNIVERSITY OF TECHNOLOGY
Gothenburg, Sweden
www.chalmers.se

CHALMERS
UNIVERSITY OF TECHNOLOGY